AMERICAN SOCIETY FOR MICROBIOLOGY | Journal of Virology®

VACCINES AND ANTIVIRAL AGENTS

Design and Characterization of Cholesterylated Peptide HIV-1/2 Fusion Inhibitors with Extremely Potent and Long-Lasting Antiviral Activity

Yuanmei Zhu,[a,b] Huihui Chong,[a,b] Danwei Yu,[a,b] Yan Guo,[c] Yusen Zhou,[c] Yuxian He[a,b]

[a]NHC Key Laboratory of Systems Biology of Pathogens, Institute of Pathogen Biology, Chinese Academy of Medical Sciences and Peking Union Medical College, Beijing, China

[b]Center for AIDS Research, Chinese Academy of Medical Sciences and Peking Union Medical College, Beijing, China

[c]Beijing Institute of Microbiology and Epidemiology, Beijing, China

ABSTRACT HIV infection requires lifelong treatment with multiple antiretroviral drugs in a combination, which ultimately causes cumulative toxicities and drug resistance, thus necessitating the development of novel antiviral agents. We recently found that enfuvirtide (T-20)-based lipopeptides conjugated with fatty acids have dramatically increased *in vitro* and *in vivo* anti-HIV activities. Herein, a group of cholesterol-modified fusion inhibitors were characterized with significant findings. First, novel cholesterylated inhibitors, such as LP-83 and LP-86, showed the most potent activity in inhibiting divergent human immunodeficiency virus type 1 (HIV-1), HIV-2, and simian immunodeficiency virus (SIV). Second, the cholesterylated inhibitors were highly active to inhibit T-20-resistant mutants that still conferred high resistance to the fatty acid derivatives. Third, the cholesterylated inhibitors had extremely potent activity to block HIV envelope (Env)-mediated cell-cell fusion, especially a truncated minimum lipopeptide (LP-95), showing a greatly increased potency relative to its inhibition on virus infection. Fourth, the cholesterylated inhibitors efficiently bound to both the cellular and viral membranes to exert their antiviral activities. Fifth, the cholesterylated inhibitors displayed low cytotoxicity and binding capacity with human serum albumin. Sixth, we further demonstrated that LP-83 exhibited extremely potent and long-lasting anti-HIV activity in rhesus monkeys. Taken together, the present results help our understanding on the mechanism of action of lipopeptide-based viral fusion inhibitors and facilitate the development of novel anti-HIV drugs.

IMPORTANCE The peptide drug enfuvirtide (T-20) remains the only membrane fusion inhibitor available for treatment of viral infection, which is used in combination therapy of HIV-1 infection; however, it exhibits relatively low antiviral activity and a genetic barrier to inducing resistance, calling for the continuous development for novel anti-HIV agents. In this study, we report cholesterylated fusion inhibitors showing the most potent and broad anti-HIV activities to date. The new inhibitors have been comprehensively characterized for their modes of action and druggability, including small size, low cytotoxicity, binding ability to human serum albumin (HSA), and, especially, extremely potent and long-lasting antiviral activity in rhesus monkeys. Therefore, the present studies have provided new drug candidates for clinical development, which can also be used as tools to probe the mechanisms of viral entry and inhibition.

KEYWORDS HIV-1, HIV-2, T-20, fusion inhibitor, lipopeptide

More than 70 million people have been infected with human immunodeficiency virus types 1 and 2 (HIV-1/2), and about half of them have died from AIDS-related illness (www.unaids.org). Because of the lack of an effective vaccine, antiviral therapy

Citation Zhu Y, Chong H, Yu D, Guo Y, Zhou Y, He Y. 2019. Design and characterization of cholesterylated peptide HIV-1/2 fusion inhibitors with extremely potent and long-lasting antiviral activity. J Virol 93:e02312-18. https://doi.org/10.1128/JVI.02312-18.

Editor Viviana Simon, Icahn School of Medicine at Mount Sinai

Address correspondence to Yuxian He, yhe@ipbcams.ac.cn.

Y.Z. and H.C. contributed equally to this work.

Received 29 December 2018
Accepted 6 March 2019
Accepted manuscript posted online 13 March 2019
Published 15 May 2019

(ART) plays important roles in both HIV treatment and prevention. Currently, the so called "U = U" strategy (undetectable = untransmittable) is highly appreciated in controlling the HIV epidemic. However, ART with multiple drugs in a combination can suppress HIV to below the detection limit, but it does not eradiate the virus, thus requiring a lifelong treatment that ultimately results in cumulative toxicities and drug resistance. Therefore, it is still imperative to develop novel agents that target different steps of the viral life cycle, including cell entry, reverse transcription, integration, and virion maturation.

Entry of HIV into target cells requires fusion of viral and cellular membranes, which is mediated by the envelope (Env) glycoproteins consisting of the surface subunit gp120 and transmembrane subunit gp41 (1, 2). Sequential binding of gp120 to the primary cell receptor CD4 and a coreceptor (CXCR4 or CCR5) can trigger conformational changes in the unmasked gp41, leading to its fusion peptide being inserted into the cell membrane. The N- and C-terminal heptad repeat regions (NHR and CHR, respectively) of gp41 transiently undergo a prehairpin intermediate (PHI) that bridges the viral and cell membranes. Subsequently, the NHR sequence forms a trimeric coiled-coil, onto which the CHR sequence folds to adopt a 6-helical bundle (6-HB) structure, driving the two membranes in close apposition for fusion. Inhibitors that bind to the PHI conformation and prevent its transition to 6-HB can competitively inhibit viral entry. Such is indeed the case for the CHR-derived peptide drug enfuvirtide (T-20) and other peptide, protein, or small molecule-based fusion inhibitors (3–6).

Approved in 2003, T-20 remains the only viral membrane fusion inhibitor available for clinical use (7–9). However, it exhibits relatively low anti-HIV activity and a genetic barrier to inducing drug resistance, which have largely limited its application. Because the deep NHR pocket is considered an ideal target site for inhibitors and the CHR-derived peptide C34 contains an N-terminal pocket-binding domain (PBD) (2, 10), a group of new fusion inhibitor peptides was previously developed with C34 as a template, such as sifuvirtide (11), SC34EK (12), and T2635 (13). Several short peptides that contain the M-T hook structure and mainly target the gp41 pocket site were also generated, such as MTSC22EK (14), HP23 (15), and 2P23 (16). The addition of a lipid group to C34, HP23, or 2P23 resulted in several lipopeptides with greatly improved pharmaceutical profiles, such as C34-Chol (17), LP-11 (18), and LP-19 (19). By contrast, little attention has been paid to the C-terminal tryptophan-rich motif (TRM) of T-20, which is considered a membrane lipid-binding domain (LBD) that can interact with the target cell membrane where fusion occurs (20–22). We recently revisited the structure and function relationship of T-20, verifying the importance of the TRM sequence for the anti-HIV activity (23, 24). By substituting the TRM sequence with a fatty acid group, we generated a T-20-based lipopeptide (LP-40) with greatly increased potency (24). It was more surprising that LP-40 could be dramatically improved by further sequence optimization, resulting in several lipopeptides that inhibited divergent HIV-1/2 and simian immunodeficiency virus (SIV) isolates at very low picomolar concentrations, including LP-50, LP-51, and LP-52 (25, 26). Very recently, a stearic acid-modified lipopeptide, termed LP-80, was generated with exceptionally potent *in vitro* inhibitory activity and *in vivo* therapeutic efficacy (27). In this study, we have designed and characterized a group of novel lipopeptide inhibitors that were conjugated with a cholesterol group.

RESULTS

Design and structural characterization of cholesterylated peptide fusion inhibitors. By adding a cholesterol group to the template peptide C34, the lipopeptide C34-Chol was reported as the most potent HIV-1 fusion inhibitor (17), and it is currently being evaluated in clinical trials (28). However, we recently found that the T-20-based sequence is a more efficient template, resulting in the inhibitors conjugated with a fatty acid group (24–27). To create an ideal candidate for clinical development and to exploit the structure-function relationship of diverse lipopeptide inhibitors, here we generated a group of T-20 backbone-based fusion inhibitors by cholesterol conjugation. As

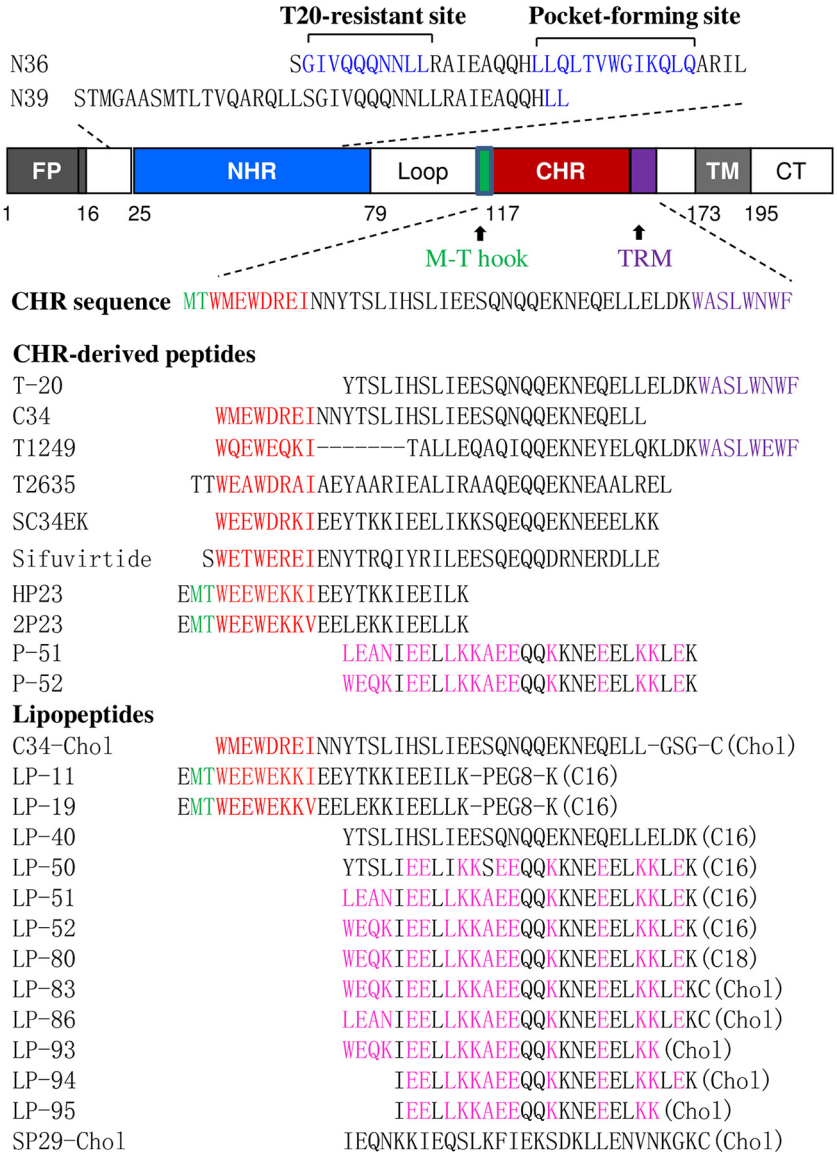

FIG 1 Schematic diagram of HIV-1 gp41 and its peptide derivatives. The gp41 numbering of HIV-1_{HXB2} is used. FP, fusion peptide; NHR, N-terminal heptad repeat; CHR, C-terminal heptad repeat; TRM, tryptophan-rich motif; TM, transmembrane domain; CT, cytoplasmic tail. The positions and sequences corresponding to the T-20-resistance mutation site and the pocket-forming site in the NHR are marked in blue. The positions and sequences of the M-T hook structure, pocket-binding domain (PBD), and tryptophan-rich motif (TRM) in the CHR are marked in green, red, and purple, respectively. Chol, C_{16}, and C_{18} in parentheses represent cholesterol, palmitic acid, and stearic acid, respectively; PEG8 represents a flexible linker of 8-unit polyethylene glycol. Engineered residues in newly designed T-20 sequence-based lipopeptides are marked in pink.

illustrated in Fig. 1, LP-83 was created by using the template peptide P-52, LP-86 used the template peptide P-51, and both of them were prepared by chemoselective thioether conjugation between the peptide sequence with an additional C-terminal cysteine residue and a cholesterol derivative. Three truncated lipopeptides (LP-93, LP-94, and LP-95) were also produced and characterized. To know their structural properties in isolation, we first applied circular dichroism (CD) spectroscopy to determine their α-helical contents and thermostabilities. As shown in Fig. 2A, LP-83 and LP-86 displayed a typical α-helical conformation with melting temperature (T_m) values of 59°C and 51°C, respectively, whereas three truncated lipopeptides exhibited dramatically reduced α-helicity, leaving their T_ms undefined. Then we analyzed the interaction

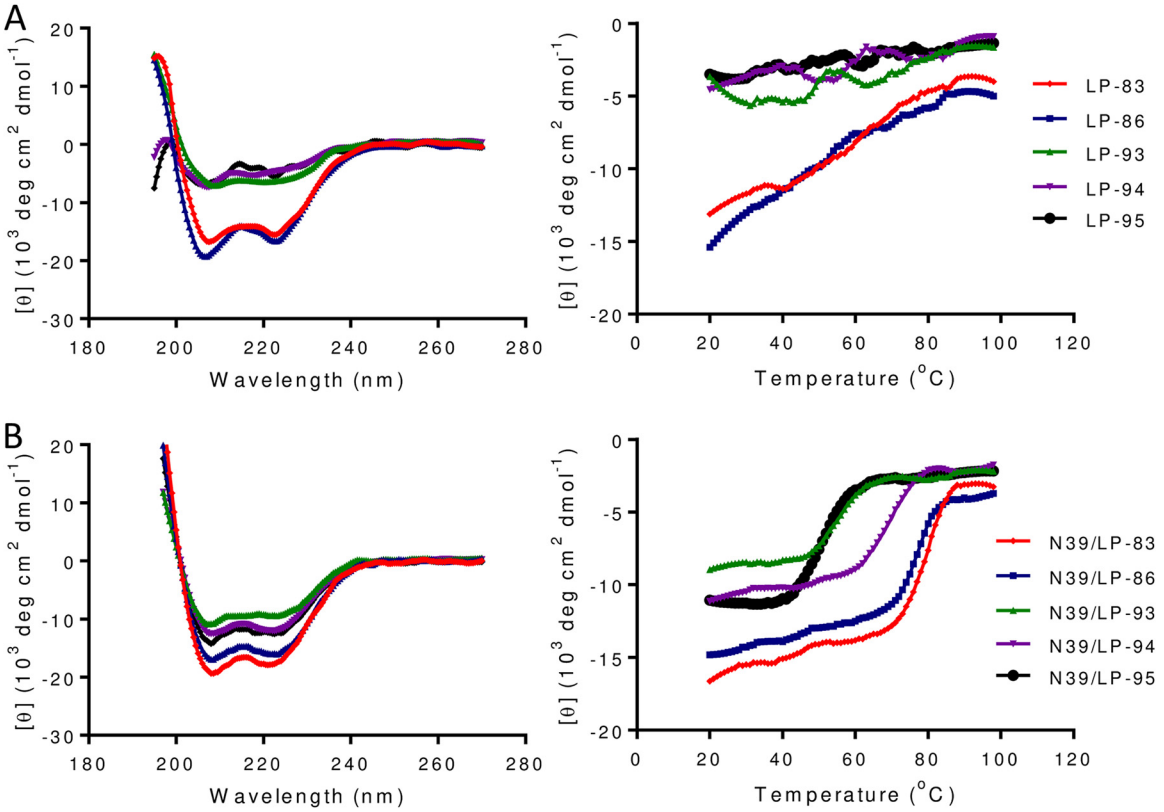

FIG 2 Secondary structure and stability of cholesterylated peptide fusion inhibitors. (A) The α-helicity (left) and thermostability (right) of inhibitors in isolation and (B) the α-helicity (left) and thermostability (right) of inhibitors in complexes with the target mimic peptide N39 were determined by CD spectroscopy. The final concentration of the isolated inhibitors was 20 μM and of the complexed inhibitors was 10 μM in PBS. The experiments were repeated 2 times, and representative data are shown.

of each lipopeptide with an NHR-derived target mimic peptide (N39) in comparison to that of T-20 and its fatty acid derivatives. As shown in Fig. 2B and Table 1, all the inhibitors interacted with N39 to form α-helical structures. The N39/LP-83 and N39/LP-86 complexes showed T_ms of 78°C and 77°C, respectively, which were comparable to that of the C_{16}-conjugated LP-52 and C_{18}-conjugated LP-80. Obviously, the N39/LP-93, N39/LP-94, and N39/LP-95 complexes had less α-helical contents with T_ms at 56°C, 67°C, and 49°C, respectively, verifying the importance of both the N-terminal (WEQK)

TABLE 1 Binding and inhibitory activities of T-20 sequence-based lipopeptide HIV fusion inhibitors[a]

Inhibitor	No. of amino acids	CD data			Mean IC_{50} ± SD (pM) for:			
		N peptide	Helix (%)	T_m (°C)	NL4-3 (X4)	JR-CSF (R5)	89.6 (R5X4)	VSV
T-20	36	N39	45	44	53,027.64 ± 6,155.69	4,468.08 ± 1,755.64	12,320.83 ± 1,863.22	>1,250,000
LP-40	28	N39	60	50	20,152.66 ± 6,125.43	1,814.52 ± 855.93	20,834.58 ± 1,261.34	>1,250,000
LP-50	28	N39	56	64	67.43 ± 15.52	23.38 ± 6.33	65.73 ± 7.71	>1,250,000
LP-51	28	N39	53	71	24.68 ± 6.34	22.75 ± 5.80	53.91 ± 9.02	>1,250,000
LP-52	28	N39	61	79	2.89 ± 1.54	8.95 ± 1.29	26.76 ± 7.42	>1,250,000
LP-80	28	N39	57	79	2.66 ± 0.76	7.12 ± 0.28	13.00 ± 4.55	>1,250,000
LP-83	29	N39	55	78	0.49 ± 0.03	4.54 ± 1.42	4.75 ± 0.83	>1,250,000
LP-86	29	N39	51	77	0.43 ± 0.03	4.78 ± 0.69	7.24 ± 1.36	>1,250,000
LP-93	25	N39	29	56	6.27 ± 1.26	6.55 ± 1.97	7.57 ± 0.62	>1,250,000
LP-94	24	N39	36	67	1.75 ± 0.23	5.90 ± 1.80	15.69 ± 1.97	>1,250,000
LP-95	21	N39	38	49	199.92 ± 32.69	24.36 ± 0.15	4,781.17 ± 699.33	>1,250,000
C34-Chol	38	N36	83	81	7.64 ± 1.76	50.86 ± 6.03	65.98 ± 7.92	>1,250,000
SP29-Chol	29	NA[b]	NA	NA	>1,250,000	>1,250,000	>1,250,000	>1,250,000
Cholesterol	NA	NA	NA	NA	>125,000,000	>125,000,000	>125,000,000	>125,000,000

[a]The anti-HIV assay was performed in triplicates and repeated three times.
[b]NA, not applicable.

and the C-terminal (LEK) residues in the α-helicity and stability of the peptide complexes. By comparing LP-93 and LP-94, the results again verified that the C-terminal motif of the lipopeptides plays a more crucial role in the inhibitor binding.

Cholesterylated inhibitors exhibit the most potent antiviral activity against divergent HIV-1 subtypes. The anti-HIV activities of cholesterylated peptides were initially evaluated with three replication-competent HIV-1 strains with different phenotypes. Herein, T-20 and its fatty acid derivatives (LP-40, LP-50, LP-51, LP-52, and LP-80) as well as C34-Chol were also included for comparison. As shown in Table 1, LP-83 and LP-86 exhibited the most potent activities in inhibiting infections of HIV-1_{NL4-3} (X4 tropic), HIV-1_{JRCSF} (R5 tropic), and HIV-$1_{89.6}$ (R5X4 tropic). For example, LP-83 and LP-86 inhibited HIV-1_{NL4-3} with mean 50% inhibitory concentrations (IC_{50}s) of 0.49 and 0.43 pM, respectively, which were >5-fold more active than LP-80 (2.66 pM), the most potent fatty acid-conjugated inhibitor being 19,935-fold more active than T-20 (53,027.64 pM). LP-83 and LP-86 inhibited HIV-1_{JRCSF} with mean IC_{50}s of 4.54 and 4.78 pM and inhibited HIV-$1_{89.6}$ with mean IC_{50}s of 4.75 and 7.24 pM, respectively, which were much lower than those of T-20 and its diverse fatty acid derivatives. Promisingly, three short cholesterol-conjugated inhibitors, especially LP-93 and LP-94, also maintained highly potent anti-HIV activities. In comparison, C34-Chol showed obviously decreased potency in inhibiting the three viruses. The anti-HIV specificity of various lipopeptide inhibitors was validated by SP29-Chol, a nonspecific peptide coupled with cholesterol in the same way as LP-83, and cholesterol alone, which did not display inhibitory activity at a concentration as high as 1.25 or 125 μM. Furthermore, no compounds showed appreciable activity in inhibiting vesicular stomatitis virus (VSV).

Next, we examined the antiviral activities of all the cholesterylated inhibitors using a large panel of HIV-1 pseudoviruses with their Envs derived from genetically different subtypes. Of them, a group of 12 Envs were reported as a "global panel" representing the worldwide HIV-1 epidemic (29). As controls, T-20, LP-52, LP-80, and C34-Chol were in parallel tested. As shown in Table 2, LP-83 and LP-86 inhibited divergent HIV-1 subtypes with mean IC_{50}s of 2.91 and 4.91 pM, respectively, while the truncated versions LP-93, LP-94, and LP-95 had mean IC_{50}s of 9.89, 6.54, and 148.88 pM, respectively. In contrast, T-20, LP-52, LP-80, and C34-Chol inhibited the same panel of viruses, with mean IC_{50}s at 34,736.67, 17.32, 5, and 65.3 pM, respectively. Therefore, LP-83 displayed slightly improved anti-HIV activity relative to LP-80, but it was 11,937-fold more active than T-20, 6-fold more active than LP-52, and 22-fold more active than C34-Chol. The antiviral activity of LP-86 was about 7,075-, 4-, and 13-fold higher than that of T-20, LP-52, and C34-Chol, respectively. Even the very short inhibitors, LP-93 (25-mer) and LP-94 (24-mer), were much more potent than T-20 (36-mer) and C34-Chol (38-mer).

Cholesterylated inhibitors exhibit extremely potent activity against T-20-resistant mutants. We previously found that fatty acid-modified inhibitors such as LP-51, LP-52, and LP-80 were highly active in inhibiting diverse HIV-1 mutants that are resistant to T-20, but these lipopeptides still displayed greatly decreased potencies relative to their inhibitions on T-20-sensitive viruses (26, 27). Therefore, we sought to characterize the newly generated cholesterol-modified inhibitors using the same panel of T-20-resistant mutants. As shown in Table 3, all the T-20-resistant mutants conferred considerable high cross-resistance to LP-80, especially those two with double mutations (NL4-$3_{I37T/N43K}$ and NL4-$3_{V38A/N42T}$). Much to our surprise, LP-83 and LP-86 maintained their extremely potent inhibitory activities against the majority of the mutant viruses. For instance, LP-83 inhibited NL4-3_{I37T} with an IC_{50} of 0.002 nM and NL4-$3_{D36S/V38M}$ with an IC_{50} of 0.005 nM, similar to its inhibitions on the T-20-sensitive (NL4-3_{D36G}) and wild-type (NL4-3_{WT}) viruses. LP-80 inhibited NL4-$3_{I37T/N43K}$ and NL4-$3_{V38A/N42T}$ with IC_{50}s of 4.006 and 3.523 nM, respectively, whereas LP-83 inhibited the two mutants with IC_{50}s of 0.041 and 0.034 nM, which indicated that LP-83 was about 98- and 104-fold more active, respectively, than LP-80. Compared to the IC_{50}s on NL4-3_{D36G}, LP-80 inhibited NL4-$3_{I37T/N43K}$ and NL4-$3_{V38A/N42T}$ with 1,335- and 1,174-fold increased IC_{50}s, whereas LP-83 only displayed 21- and 17-fold changes, respectively. As expected, C34-Chol

TABLE 2 Inhibitory activities of lipopeptide fusion inhibitors on divergent HIV-1 subtypes[a]

Pseudovirus	Subtype	Mean IC_{50} ± SD (pM) for:								
		T-20	LP-52	LP-80	LP-83	LP-86	LP-93	LP-94	LP-95	C34-Chol
92RW020	A	3,798 ± 190.48	38.54 ± 9.18	9.09 ± 0.91	4.52 ± 0.48	5.99 ± 1.9	15.18 ± 1.15	10.18 ± 2.41	187.29 ± 101.8	90.02 ± 8.72
92UG037.8	A	6,601.33 ± 572	26.53 ± 1.94	3.28 ± 0.62	4.14 ± 0.71	4.22 ± 1.49	25.62 ± 6.75	20.92 ± 0.54	54.25 ± 5.75	116.44 ± 20.51
398-F1_F6_20[b]	A	21,653.33 ± 3,381.83	10.39 ± 1.4	1.54 ± 0.07	1.23 ± 0.23	1.37 ± 0.26	2.98 ± 0.04	1.26 ± 0.65	23.42 ± 1	14.97 ± 1.88
PVO	B	65,066.67 ± 5,256.24	33.01 ± 4.62	11.05 ± 2.72	3.61 ± 0.58	7.43 ± 2.5	20.29 ± 12.56	5.67 ± 2.06	101.98 ± 37.93	106.22 ± 11.67
pREJO4541	B	53,141.67 ± 4,642.64	8.77 ± 1.21	1.15 ± 0.35	4.68 ± 0.26	4.74 ± 2.27	15.10 ± 3.03	8.79 ± 2.35	1,148.57 ± 271.92	66.52 ± 9.46
SF162	B	15,646 ± 2,881.32	13.18 ± 0.41	4.15 ± 2.48	1.75 ± 0.5	2.14 ± 0.52	5.70 ± 0.53	3.05 ± 0.14	25.61 ± 2.97	32.41 ± 1.83
JRFL	B	9,887.33 ± 474.31	45.19 ± 4.78	9.31 ± 1.61	3.50 ± 0.55	4.67 ± 0.38	8.23 ± 0.95	4.3 ± 0.95	24.89 ± 0.73	115.2 ± 7.29
SC422661.8	B	14,668.67 ± 1,976.15	6.64 ± 0.87	1.92 ± 0.89	3.29 ± 0.48	5.76 ± 1.71	12.47 ± 2.93	6.01 ± 0.12	1,203.33 ± 122.98	73.39 ± 9.22
AC10.0.29	B	2,947.67 ± 585.03	8.50 ± 1.83	4.84 ± 0.81	1.95 ± 0.51	5.14 ± 0.76	8.98 ± 6.49	4.63 ± 2.93	17.81 ± 1.34	34.72 ± 4.76
TRO.11[b]	B	6,550.67 ± 902.82	18.49 ± 4.18	3.44 ± 0.68	1.35 ± 0.47	2.45 ± 0.11	6.1 ± 1.32	2.85 ± 1.17	66.65 ± 25.43	28.73 ± 2.03
X2278_C2_B6[b]	B	5,412.33 ± 275.16	7.64 ± 2.6	0.6 ± 0.46	1.76 ± 0.94	0.77 ± 0.06	3.24 ± 0.78	2.38 ± 0.08	36.17 ± 21.04	9.22 ± 2.32
R3A	B	7,497 ± 572.5	12.52 ± 3.35	5.67 ± 1.14	2.48 ± 0.47	4.31 ± 0.09	3.97 ± 0.52	6.83 ± 1.02	77.94 ± 17.99	42.79 ± 16.02
B01	B′	77,094.33 ± 1,690.12	12.1 ± 1.41	3.77 ± 0.41	3.87 ± 0.97	6.36 ± 1.72	7.31 ± 0.54	6.84 ± 2.82	200.37 ± 89.2	46.31 ± 7.22
B02	B′	12,801 ± 1,161.16	9.96 ± 1.08	8.22 ± 0.95	3.51 ± 0.23	6.14 ± 1.59	8.74 ± 1.61	6.45 ± 2.18	191.33 ± 24.13	61.34 ± 8.79
B04	B′	5,514 ± 388.23	7.86 ± 1.31	4.31 ± 1.54	2.79 ± 0.28	6.38 ± 0.32	3.66 ± 0.19	2.6 ± 0.08	397.1 ± 43.2	77.86 ± 10.18
43-22	B′	16,565 ± 1,544.92	5.89 ± 1.07	2.18 ± 1.06	2.19 ± 1.24	3.54 ± 0.71	4.05 ± 1.6	4.81 ± 3.56	41.01 ± 21.5	25.76 ± 5.66
Du156	C	15,732.67 ± 1,334.81	7.01 ± 2.14	2.04 ± 0.68	1.72 ± 0.37	2.30 ± 0.26	3.98 ± 0.54	2.71 ± 0.66	104.38 ± 5.31	26.95 ± 2.13
ZM53M.PB12	C	23,173.33 ± 2,129.02	16.55 ± 3.86	7.27 ± 1.83	4.19 ± 0.78	4.59 ± 0.69	10.60 ± 0.93	7.13 ± 2.6	119.58 ± 83.57	83.42 ± 8.69
CAP210.2.00.E8	C	163,602 ± 16,751.97	29.71 ± 6.17	10.47 ± 0.2	3.69 ± 0.1	6.55 ± 1.96	13.39 ± 7.23	7.75 ± 3.36	309.59 ± 160.39	77.8 ± 10.85
CAP45.2.00.G3	C	111,593.33 ± 16,592.38	7.87 ± 2.35	3.02 ± 1.73	1.45 ± 0.51	1.24 ± 0.16	5.62 ± 3.41	2.62 ± 0.89	13.31 ± 2.76	10.95 ± 1.55
CE703010217_B6[b]	C	44,885.33 ± 1,800.47	11.92 ± 3.02	4.45 ± 1.8	1.70 ± 0.42	3.42 ± 0.3	10.16 ± 3.57	4.73 ± 0.69	36.52 ± 4.59	83.22 ± 10.65
HIV_25710-2.43[b]	C	13,219.67 ± 2,638.09	19.47 ± 2.7	3.40 ± 0.28	2.28 ± 0.44	3.34 ± 1.06	7.76 ± 1.74	6.12 ± 0.23	118.50 ± 51.16	47.28 ± 6.71
CE1176_A3[b]	C	8,452 ± 804.32	12.77 ± 5.33	2.25 ± 0.98	4.03 ± 0.67	5.13 ± 1.06	11.45 ± 2.3	9.66 ± 2.57	38.97 ± 2.86	82.73 ± 3.01
X1632-S2-B10[b]	G	17,464.33 ± 1,656.28	24.92 ± 1.01	3.90 ± 2.35	2.60 ± 0.44	5.67 ± 1.78	8.28 ± 1.66	7.21 ± 1.16	46.22 ± 19.01	92.06 ± 9.06
246_F3_C10_2[b]	A/C	36,237 ± 1,246.91	14.28 ± 2.11	4.87 ± 2.34	1.68 ± 0.18	2.41 ± 0.35	3.76 ± 0.22	2.71 ± 0.41	12.34 ± 1.77	40.04 ± 2.91
AE03	A/E	16,585.33 ± 2,284.25	13.26 ± 1.34	2.72 ± 1.29	1.80 ± 0.75	3.14 ± 0.13	3.30 ± 1.29	3.24 ± 1.99	180.97 ± 31.35	16.39 ± 4.91
GX11.13	A/E	30,265.67 ± 2,927.55	8.93 ± 1.13	5.35 ± 0.7	3.80 ± 0.41	8.04 ± 2.14	11.59 ± 0.76	14.78 ± 2.28	52.58 ± 25.92	141.57 ± 20.12
SHX335.24	A/E	37,818.33 ± 2,638.78	20.64 ± 3.82	5 ± 2.74	1.73 ± 0.62	2.44 ± 0.62	5.61 ± 0.43	2.16 ± 1.05	21.33 ± 2.62	47 ± 4.71
CNE8[b]	A/E	22,938± 2,408.89	9.57 ± 2.59	7.13 ± 4.21	5.06 ± 0.4	7.23 ± 1.48	12.57 ± 1.24	23.22 ± 8.15	108.34 ± 16.64	113.75 ± 5.16
CNE55[b]	A/E	27,066± 1,864.23	13.4 ± 4.37	1.48 ± 0.53	1.93 ± 0.7	5.28 ± 0.41	5.54 ± 2.39	3.27 ± 1.29	15.60 ± 4.86	39.37 ± 5.66
CH64.20	B/C	33,537.33 ± 3,582.23	33.23 ± 1.79	8.86 ± 4.39	4.42 ± 2.71	4.07 ± 0.97	9.73 ± 7.28	5.49 ± 4.5	25.99 ± 5.11	42.62 ± 2.97
CH070.1	B/C	205,182.67 ± 3,509.09	38.19 ± 3.78	12.34 ± 8.06	4.25 ± 0.6	13.38 ± 0.06	27.92 ± 5.84	11.55 ± 0.29	105.42 ± 17.88	212.54 ± 12.73
CH110	B/C	32,772.67 ± 1,753.18	12.57 ± 1.37	3.3 ± 0.01	2.79 ± 0.86	4.65 ± 1.06	10.22 ± 3.84	5.87 ± 0.09	51.29 ± 28.55	41.08 ± 1.65
CH119.10[b]	B/C	43,322.67 ± 2,147.37	11.81 ± 2.8	4.05 ± 0.93	2.35 ± 0.35	1.95 ± 0.07	7.03 ± 1.1	5.19 ± 0.98	63.80 ± 8.8	41.04 ± 4.18
CH120.6	B/C	14,702.33 ± 2,251.62	18.83 ± 1.9	7.96 ± 3.5	4.53 ± 1.36	14.42 ± 1.28	26 ± 5.13	17.34 ± 0.26	67.34 ± 24.52	101.34 ± 8.58
BJOX002000.03.2[b]	B/C	27,124.33 ± 4,319.36	33.28 ± 4.21	5.51 ± 2.53	2.14 ± 0.73	6.02 ± 0.25	9.9 ± 1.41	5.12 ± 0.6	70.04 ± 29.5	67.89 ± 5.65
Mean		34,736.67	17.32	5	2.91	4.91	9.89	6.54	148.88	65.3

[a]The assay was performed in triplicates and repeated three times.
[b]The global panel of HIV-1 Envs.

TABLE 3 Inhibitory activity of lipopeptide fusion inhibitors on T-20-resistant HIV-1 mutants and HIV-2 and SIV isolates[a]

Virus	Mean IC_{50} ± SD (nM) for:							
	T-20	LP-80	LP-83	LP-86	LP-93	LP-94	LP-95	C34-Chol
T-20 sensitive								
NL4-3_{D36G}	8.564 ± 1.045	0.003 ± 0.001	0.002 ± 0	0.003 ± 0	0.006 ± 0.001	0.004 ± 0.002	0.067 ± 0.026	0.012 ± 0.001
T-20 resistant								
NL4-3_{WT}	169.333 ± 2.559	0.007 ± 0.002	0.002 ± 0.001	0.003 ± 0	0.012 ± 0.001	0.006 ± 0	0.39 ± 0.016	0.029 ± 0.001
NL4-3_{I37T}	1,256.333 ± 54.501	0.121 ± 0.022	0.002 ± 0	0.004 ± 0	0.019 ± 0.002	0.004 ± 0	3.541 ± 0.307	0.042 ± 0.005
NL4-3_{V38A}	2,268 ± 41.581	0.551 ± 0.071	0.008 ± 0.001	0.028 ± 0.008	0.045 ± 0.004	0.061 ± 0.001	9.432 ± 1.999	0.034 ± 0.014
NL4-3_{V38M}	1,056 ± 44.643	0.262 ± 0.014	0.004 ± 0	0.014 ± 0.002	0.024 ± 0.003	0.031 ± 0.007	8.362 ± 3.532	0.044 ± 0.018
NL4-3_{Q40H}	1,232.333 ± 97.992	0.325 ± 0.048	0.004 ± 0	0.011 ± 0.002	0.117 ± 0.024	0.018 ± 0.007	41.599 ± 1.56	0.038 ± 0.007
NL4-3_{N43K}	794.667 ± 102.762	0.535 ± 0.028	0.009 ± 0.001	0.023 ± 0.004	0.267 ± 0.005	0.196 ± 0.007	57.802 ± 3.762	0.039 ± 0.006
NL4-$3_{G36S/V38M}$	317.333 ± 18.728	0.209 ± 0.008	0.005 ± 0	0.012 ± 0.001	0.012 ± 0.003	0.0267 ± 0.003	3.828 ± 0.172	0.06 ± 0.014
NL4-$3_{I37T/N43k}$	7,901± 1,091.948	4.006 ± 0.367	0.041 ± 0.004	0.124 ± 0.011	2.17 ± 0.135	2.295 ± 0.456	408.556 ± 12.919	0.047 ± 0.015
NL4-$3_{V38A/N42T}$	6,260.333 ± 121.467	3.523 ± 0.195	0.034 ± 0.003	0.17 ± 0.046	0.34 ± 0.027	0.243 ± 0.059	82.514 ± 3.259	0.034 ± 0.003
HIV-2/SIV								
HIV-2_{ROD}	341.508 ± 130.145	0.288 ± 0.103	0.032 ± 0.005	0.026 ± 0.004	3.514 ± 0.907	0.019 ± 0.006	13.512 ± 1.881	0.929 ± 0.033
HIV-2_{ST}	630.633 ± 84.581	0.299 ± 0.081	0.02 ± 0.008	0.014 ± 0.007	1.244 ± 0.079	0.027 ± 0.006	2.857 ± 0.541	0.53 ± 0.028
SIV_{239}	534.33 ± 83.53	0.034 ± 0.002	0.004 ± 0	0.005 ± 0.001	0.013 ± 0.048	0.018 ± 0.002	0.862 ± 0.069	0.078 ± 0.009
SIV_{PBJ}	915.516 ± 104.294	0.155 ± 0.06	0.006 ± 0.001	0.006 ± 0.002	0.773 ± 0.036	0.011 ± 0.002	0.556 ± 0.08	1.605 ± 0.421

[a]The assay was performed in triplicates and repeated three times.

showed mild cross-resistance (3- to 5-fold) on diverse T-20-resistant mutants. With respect to LP-83, C34-Chol showed similar activities on NL4-$3_{I37T/N43K}$ and NL4-$3_{V38A/N42T}$, but it was much less active (4- to 21-fold) in inhibiting other mutants tested. Furthermore, the C-terminal truncated LP-93 and the N-terminal truncated LP-94 also displayed highly potent activities against T-20-resistant mutants, but the results verified that both the terminal motifs contributed critically to the potency of LP-83 or LP-86.

Cholesterylated inhibitors exhibit extremely potent activity against HIV-2 and SIV isolates. In the previous works, we also demonstrated that the fatty acid-conjugated inhibitors possess highly potent activity against HIV-2 and SIV isolates (25–27). Here, we also characterized the inhibitory activities of cholesterol-modified inhibitors in comparison to T-20, LP-80, and C34-Chol. As shown in Table 3, T-20 exhibited very low activities in inhibiting two HIV-2 isolates (ROD and ST) and two SIV isolates (239 and PBJ). By contrast, LP-80 was highly active on these viruses; however, LP-83 and LP-86 were much more potent than LP-80. For instance, LP-83 inhibited HIV-2_{ROD} and HIV-2_{ST} with IC_{50}s of 0.032 and 0.02 nM, which were 9- and 15-fold lower than that of LP-80, respectively; LP-83 inhibited SIV_{239} and SIV_{PBJ} with IC_{50}s of 0.004 and 0.006 nM, which were 9- and 26-fold lower than that of LP-80, respectively. Compared to C34-Chol, LP-83 was 29-, 27-, 20-, and 268-fold more potent in inhibiting HIV-2_{ROD}, HIV-2_{ST}, SIV_{239}, and SIV_{PBJ}, respectively. Even the truncated LP-94, with a 24-amino-acid sequence, was much more active than LP-80 and C34-Chol. By comparing the activities of three truncated inhibitors, it is obvious that the C-terminal motif of cholesterylated inhibitors contributed more critically than the N-terminal motif in the inhibitions of the HIV-2 and SIV viruses.

Cholesterylated inhibitors possess extremely potent activities on Env-mediated cell-cell fusion. To explore the mechanism underlying the extremely potent antiviral activities of the newly developed lipopeptide inhibitors, we sought to characterize their inhibitory activities on HIV Env-mediated cell-cell fusion. To this end, a dual-split-protein (DSP)-based cell-cell fusion assay was applied, in which an Env-expressing plasmid along with a DSP_{1-7}-expressing plasmid was transfected into HEK293T as effector cells and then incubated with HEK293T expressing CCR5/CXCR4 and DSP_{8-11} as target cells. As shown in Table 4, all the new lipopeptide inhibitors exhibited highly potent activities in blocking diverse Env-mediated cell-cell fusion, with mean IC_{50}s in the very low picomolar range. Specifically, the fatty acid derivatives LP-52 and LP-80 had IC_{50}s of 56.67 and 13.4 pM, respectively, the new cholesterol derivatives LP-83,

TABLE 4 Inhibitory activity of lipopeptide fusion inhibitors on HIV-1 Env-mediated cell-cell fusion[a]

Env	Subtype	Mean IC_{50} ± SD (pM) for:								
		T20	LP-52	LP-80	LP-83	LP-86	LP-93	LP-94	LP-95	C34-Chol
92RW020	A	788.87 ± 39.86	159.53 ± 15.81	5.07 ± 0.53	6.4 ± 1	7.78 ± 0.9	12.19 ± 2.43	16.24 ± 3.61	18.1 ± 2.56	44.11 ± 9.17
PVO	B	6,268.67 ± 1,763.06	129.1 ± 19.93	9.52 ± 2.22	5.27 ± 0.72	7.6 ± 1.06	8.3 ± 1.01	17.14 ± 2.26	16.42 ± 5.11	47.21 ± 9.06
B02	B′	14,783.33 ± 1,955.25	47.63 ± 4.8	26.15 ± 2.89	10.07 ± 1.41	18.11 ± 1.57	26.16 ± 5.99	30.65 ± 3.81	54.18 ± 9.6	243.77 ± 35.87
CAP210.2.00.E8	C	4,311.67 ± 518.8	21.08 ± 1.93	15.04 ± 2.63	6.61 ± 0.89	8 ± 0.85	12.17 ± 1.67	16.44 ± 1.95	18.24 ± 1.78	142.3 ± 33.46
X1632-S2-B10	G	10,708 ± 1,666.1	21.17 ± 8.85	7.6 ± 1.05	4.67 ± 1.11	4.02 ± 1.29	9.53 ± 2.23	8.45 ± 2.88	25.16 ± 5.68	153.97 ± 36.72
246F3	A/C	11,330 ± 1,156.26	5.05 ± 0.7	9.78 ± 0.94	4.53 ± 0.77	6.1 ± 1.54	10.37 ± 0.9	11.11 ± 1.93	13.72 ± 2.63	97.5 ± 4.86
GX11.13	A/E	9,439 ± 2,593.64	42.34 ± 2.2	20.45 ± 2.55	14.35 ± 1.01	22.99 ± 1.78	16.22 ± 1.77	51.96 ± 14.35	31.89 ± 3.91	229.9 ± 10.34
CH120.6	B/C	11,422 ± 2,323.97	27.45 ± 4.69	13.57 ± 3.07	16.47 ± 3.05	23.59 ± 5.82	21.15 ± 1.68	66.9 ± 3.61	61.03 ± 9.05	190.1 ± 66.12
Mean		8,631.44	56.67	13.4	8.55	12.27	14.51	27.36	29.84	143.61

[a]The assay was performed in triplicates and repeated three times.

LP-86, LP-93, LP-94, and LP-95 had IC_{50}s of 8.55, 12.27, 14.51, 27.36, and 29.84 pM, respectively. Compared to T-20 and C34-Chol, both the fatty acid and cholesterol derivatives exhibited markedly increased potencies. Interestingly, with respect to its inhibitions on the infectious clones and the panel of pseudoviruses shown in Tables 1 and 2, the minimum lipopeptide LP-95 inhibited cell-cell fusion more efficiently. In comparison, the mean IC_{50} of LP-95 on divergent pseudoviruses was 51-fold higher than that of LP-83, but its mean IC_{50} on cell-cell fusion was only 3-fold higher than that of LP-83; while LP-95 was >2-fold less potent than C34-Chol on the pseudoviruses, it was about 5-fold more potent than C34-Chol on cell-cell fusion.

Cholesterylated inhibitors can efficiently bind to cellular and viral membranes. Lipopeptide-based viral fusion inhibitors are considered to bind preferentially with the target cell membranes where fusion occurs, thus raising the local concentration of the inhibitors (17, 30–33). By using physical and functional approaches, we previously observed that LP-52 could efficiently bind and accumulate in the target cell membrane (26). Herein, we were interested in characterizing the cell membrane-binding abilities of diverse lipopeptides in comparison to those of T-20, C34, and the template peptide P-52. To this end, all the inhibitors were preincubated with TZM-bl cells, followed by thorough washing to remove unbound inhibitors. The virus was then added to initiate infection, and the antiviral activities of the membrane-bound inhibitors that survived the washing steps were determined. As shown in Fig. 3A and B, the unconjugated T-20, C34, and P-52 had dramatically reduced activities in inhibiting HIV-1_{NL4-3} and HIV-1_{JRCSF} infections; however, the inhibitory activities of all the lipopeptide inhibitors were largely sustained. Compared to that with the fatty acid derivatives LP-52 and LP-80, the cholesterylated inhibitors LP-83 and LP-86 attached to the cell membrane more efficiently. We next determined the IC_{50}s of LP-83 and LP-86 with or without the washing (Fig. 3C to F). It was found that the membrane-bound LP-83 and LP-86 still inhibited HIV-1_{NL4-3} with IC_{50}s of 11.62 and 10.57 pM, respectively, and inhibited HIV-1_{JRCSF} with IC_{50}s of 131.23 and 114.63 pM, respectively. In parallel, LP-83 and LP-86, without the washing steps, inhibited HIV-1_{NL4-3} with IC_{50}s of 0.42 and 0.43 pM, respectively, and inhibited HIV-1_{JRCSF} with IC_{50}s of 4.71 and 5.15 pM, respectively. Furthermore, the lipopeptides that bound to the cell membrane were physically visualized by fluorescein isothiocyanate (FITC)-labeled inhibitors (Fig. 4). Similarly to the functional assays described above, the FITC-labeled inhibitors were preincubated with target cells, followed by thorough washing, and their membrane-binding abilities were observed by fluorescence microscopy. As a control (Fig. 4A), FITC-labeled P-52 was not observed at a concentration as high as 50 μM, whereas three FITC-labeled lipopeptides (LP-52, LP-80, and LP-83) accumulated at the cell surface in a dose-dependent manner (Fig. 4B to D). In comparison, LP-83 displayed the strongest fluorescence intensities, suggesting that it attached to the cell membrane more effectively.

We also sought to characterize the binding and inhibitory abilities of inhibitors with viral membrane. For this, the inhibitors were preincubated with a virus, and the unbound ones were removed by precipitating the virus with polyethylene glycol 6000 (PEG 6000). The antiviral activities of the virus-bound inhibitors were similarly deter-

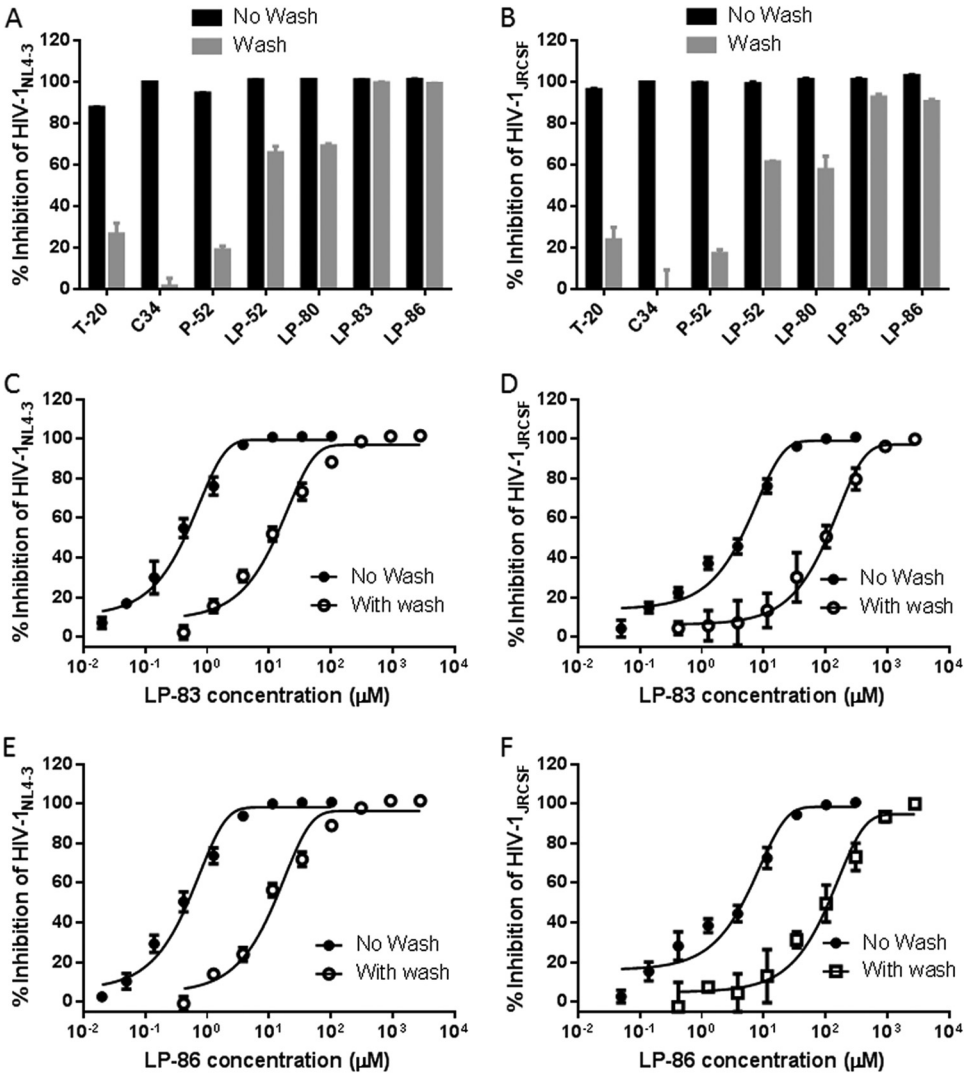

FIG 3 Binding ability of fusion inhibitors with the target cell membrane. The lipopeptide inhibitors LP-52, LP-80, LP-83, and LP-86 and the control inhibitors T-20, C34, and P-52 were preincubated with TZM-b1 cells, followed by thorough washes, and their sustained activities in inhibiting the infectious molecular clones HIV-1_{NL4-3} (A) and HIV-1_{JRCSF} (B) were measured. LP-52, LP-80, LP-83, and LP-86 were used at 0.5 nM, while T-20, C34, and P-52 were used at 750, 25, and 200 nM, respectively. (C to F) The IC_{50} values of LP-83 and LP-86, administered with or without the washing steps, on HIV-1_{NL4-3} and HIV-1_{JRCSF} were determined. The experiments were performed 3 times, and data are expressed as means ± standard deviations (SDs).

mined. As shown in Fig. 5A and B, all the lipopeptides maintained their potent anti-HIV activities, and they bound to the X4-tropic virus HIV-1_{NL4-3} more efficiently than to the R5-tropic virus HIV-1_{JRCSF}. Then, we measured the IC_{50}s of LP-83 and LP-86 administered with or without the washing steps (Fig. 5C to F). The virus-bound LP-83 and LP-86 inhibited HIV-1_{NL4-3}, with IC_{50}s of 196.3 and 112.32 pM and HIV-1_{JRCSF} with IC_{50}s of 741.83 and 1,463.67 pM, respectively; by contrast, the unwashed LP-83 and LP-86 inhibited HIV-1_{NL4-3} with IC_{50}s of 0.57 and 0.53 pM and HIV-1_{JRCSF} with IC_{50}s of 5.54 and 5.55 pM, respectively. Taken together, the results suggested that lipopeptide-based fusion inhibitors can bind to both the cellular and viral membranes that might contribute the antiviral activity synergistically.

Cholesterylated inhibitors can efficiently bind to human serum albumin. LP-52 was also found to bind to human serum albumin (HSA) in a dose-dependent manner, which should correlate with its *in vivo* stability (26). In this study, we were interested in characterizing the binding abilities of cholesterylated inhibitors with HSA in compari-

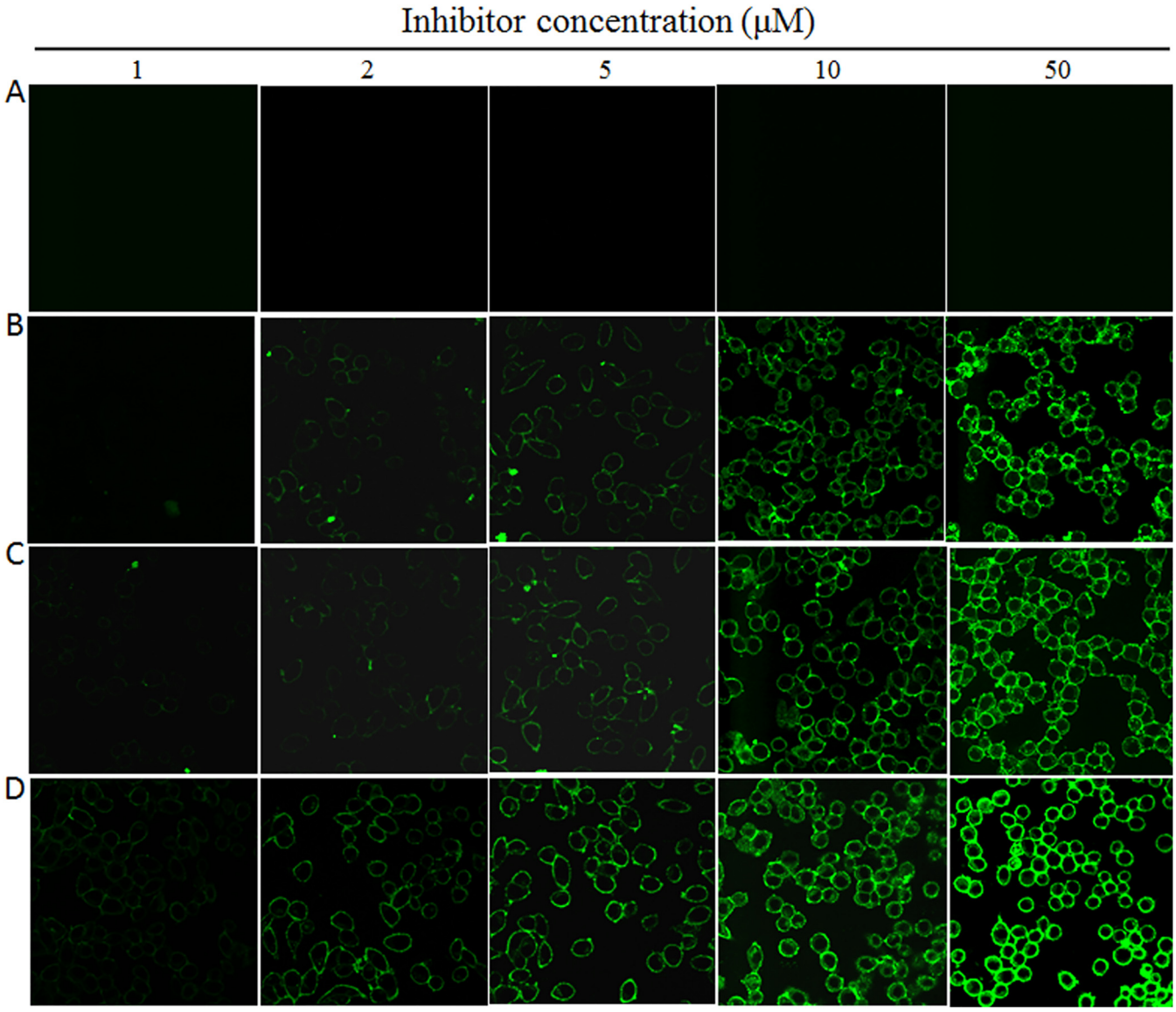

FIG 4 Visualization of lipopeptide inhibitors bound to the target cell membrane. Different concentrations of FITC-labeled P-52 (A), LP-52 (B), LP-80 (C), and LP-83 (D) were preincubated with TZM-b1 cells for 30 min, followed by washes, and the fluorescence intensities of membrane-attached inhibitors were observed under a confocal microscope.

son to the fatty acid-conjugated peptides. First, the reactivity of diverse inhibitors with the mouse monoclonal antibody 12H1 was identified by enzyme-linked immunosorbent assay (ELISA). As shown in Fig. 6A, P-52, LP-52, and LP-80 strongly reacted with 12H1, whereas LP-83 and LP-94 had relatively decreased reactivity. Considering that LP-93 and LP-95 could not be recognized by 12H1, the C-terminal sequence of the inhibitors critically determined the antibody epitope. Next, we used 12H1 to detect the binding abilities of P-52, LP-52, LP-80, LP-83, and LP-94. As shown in Fig. 6B, both the fatty acid- and cholesterol-conjugated inhibitors showed dose-dependent binding, in sharp contrast to the template peptide P-52. In terms of their reactivity, LP-83 bound to HSA more efficiently than LP-52, while LP-83 and LP-80 might have similar binding capacities. We were intrigued to know whether the inhibitors that bound to HSA were still antivirally active. To this end, the lipopeptides were incubated with a final concentration of 20% HSA at 37°C for 30 min, and their anti-HIV activities were then measured. As demonstrated by the IC_{50} values in Fig. 6C and D, the addition of HSA did not affect the ability of the inhibitors to inhibit both HIV-1_{NL4-3} and HIV-1_{JRCSF} isolates.

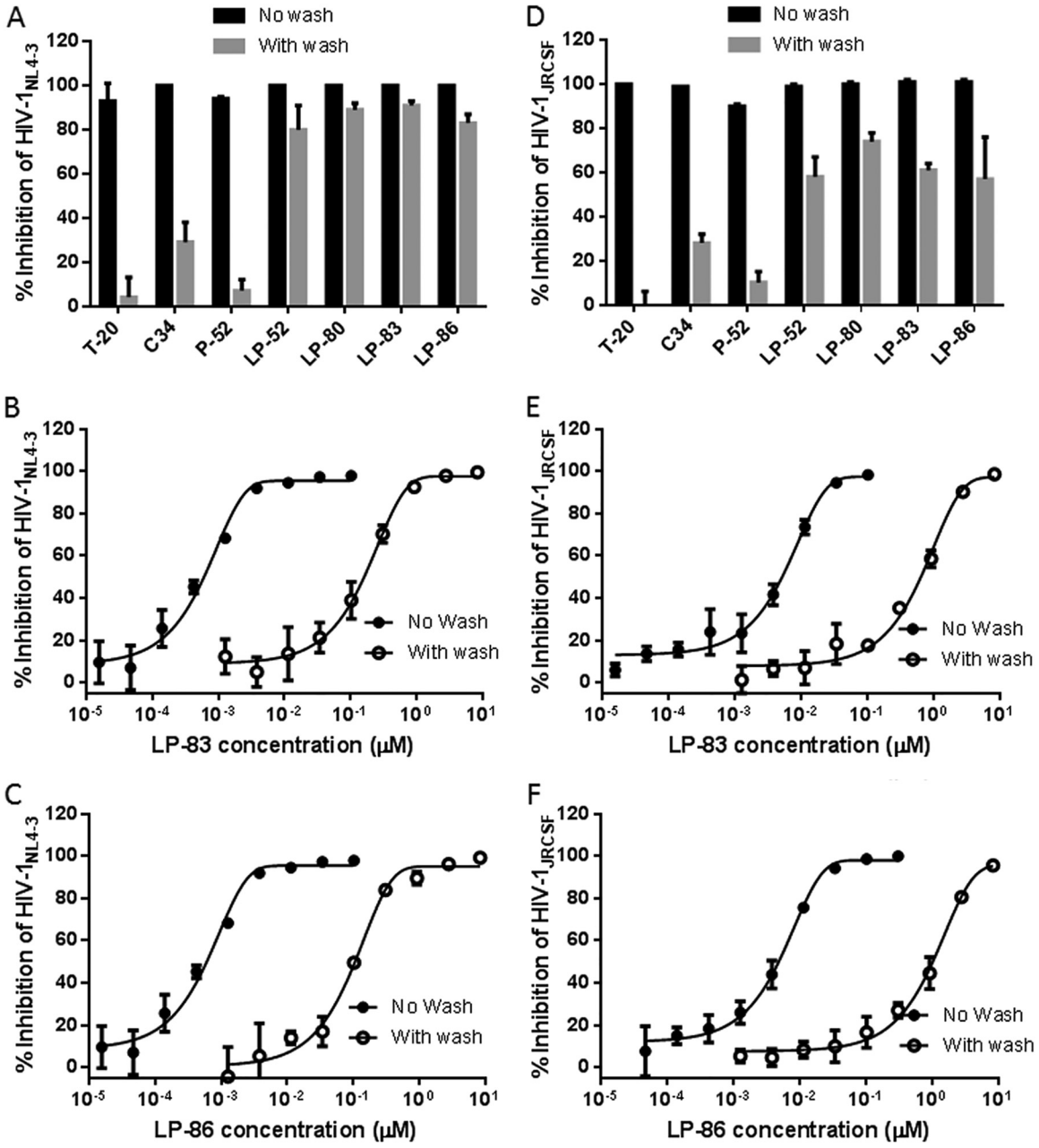

FIG 5 Binding ability of fusion inhibitors with the viral membrane. All the inhibitors were preincubated with the infectious virus HIV-1_{NL4-3} (A) or HIV-1_{JRCSF} (B). After thorough washes, the antiviral activities of the virus-bound inhibitors were measured. LP-52, LP-80, LP-83, and LP-86 were used at 0.5 nM, while T-20, C34, and P-52 were used at 250, 25, and 25 nM, respectively. (C to F) The IC_{50} values of LP-83 and LP-86, administered with or without the washing steps, on HIV-1_{NL4-3} and HIV-1_{JRCSF} were determined. The experiments were performed 3 times, and data are expressed as means ± SDs.

LP-83 exhibits very low cytotoxicity and a high therapeutic selectivity index. We previously reported that T-20 derivatives, such as LP-50, LP-51, LP-52, and LP-80, possess extremely low cytotoxicity and high genetic resistance barriers (26, 27). Because LP-83 exhibited the most potent antiviral activity, here we focused on characterizing its cytotoxicity in different cell lines and human peripheral blood mononuclear cells (PBMCs). It was found that LP-83 had a 50% cytotoxic concentration (CC_{50}) of 12.34 μM in TZM-bl cells, of 19.65 μM in MT-4 cells, of 19.19 μM in C8166 cells, of 9.97 μM in U937 cells, of 25.31 μM in HEK293T cells, and of 40.27 μM in human PBMCs. Considering its antiviral potency, the presented results suggested that LP-83 possesses

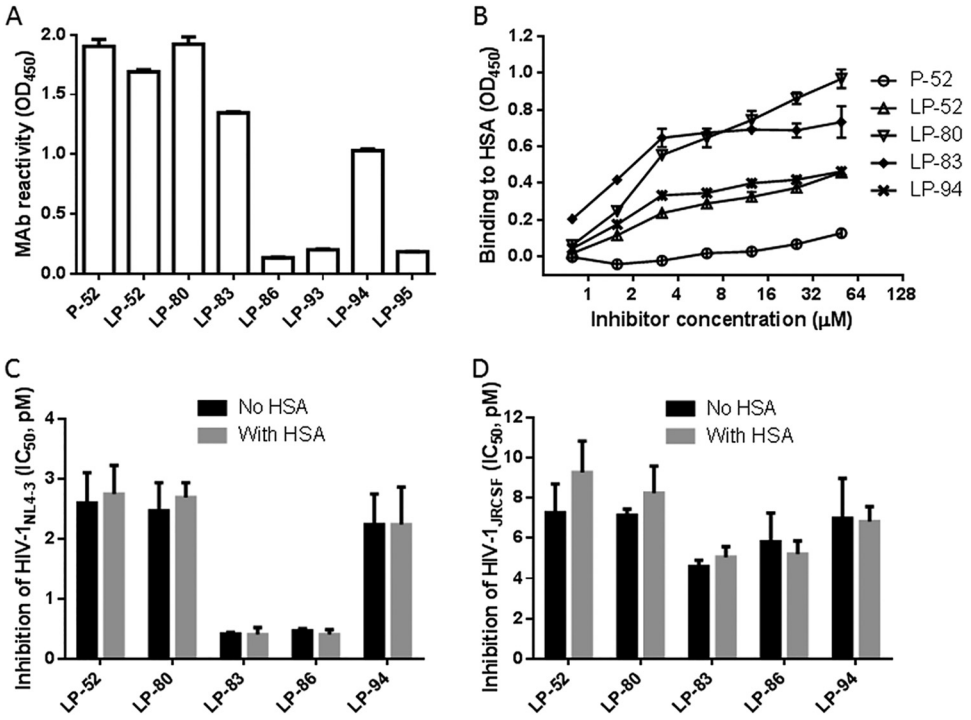

FIG 6 Binding ability of lipopeptide inhibitors with human serum albumin. (A) Reactivity of diverse lipopeptide inhibitors with the mouse anti-P52 monoclonal clonal antibody 12H1 in ELISA. A lipopeptide was precoated on the ELISA plate well, and 12H1 was tested at 10 μg/ml. (B) Different concentrations of P-52, LP-52, LP-80, LP-83, or LP-94 were incubated with precoated HSA, followed by washes, and bound inhibitors were detected by 12H1 antibody and HRP-conjugated anti-mouse IgG. (C) The inhibitory activities of lipopeptides on HIV-1_{NL4-3} in the presence and absence of HSA. (D) The inhibitory activities of lipopeptides on HIV-1_{JRCSF} in the presence and absence of HSA.

an extremely high therapeutic selectivity index (CC_{50}/IC_{50} ratio). However, the cytotoxicity of LP-83 is relatively higher than those of the fatty acid-conjugated inhibitors determined previously (26, 27).

LP-83 exhibits the most potent and long-acting *ex vivo* anti-HIV activity. We previously evaluated the antiviral activities of T-20, LP-19, LP-40, LP-50, and LP-51 in a nonhuman primate model (19, 25). Herein, we focused on comparing the *in vivo* activities and stabilities of three classes of the lipopeptide inhibitors, including the C_{16} fatty acid-conjugated LP-52, the C_{18} fatty acid-conjugated LP-80, and the cholesterol-conjugated LP-83, which share the same template peptide sequence (P-52). Each lipopeptide was subcutaneously injected into six rhesus monkeys at a dosage of 3 mg/kg of body weight. The pharmacological kinetics of the inhibitors in monkey sera were measured pre- or postadministration, which could reflect their *in vivo* antiviral activities and half-lives. As shown in Fig. 7A, LP-52 reached a serum peak level 4 h after injection, with a dilution of 700,802-fold that inhibited 50% of virus infection, similar to that of the C_{16}-conjugated lipopeptides LP-50 and LP-51, determined previously (25). After injection, at 72 h, the inhibitory activity of LP-52 in the sera declined to a low level, as indicated by a 182-fold serum dilution. LP-80 reached a serum peak level 8 h after injection, with a serum dilution of 589,867-fold (Fig. 7B). However, the inhibitory activity of LP-80 was maintained at a very high level 72 h after injection (the serum dilution was 13,208-fold) and persisted until 168 h (the serum dilution was 73-fold). In sharp contrast, LP-83 maintained its serum peak level between 8 and 48 h after injection, and the dilutions ranged from 412,583- to 452,629-fold. After 72 h and 168 h, the serum dilutions that inhibited 50% of virus infection remained at 164,646- and 2,229-fold, respectively (Fig. 7C). Because the same group of six monkeys was previously used for T-20, LP-19, LP-40, LP-50, and LP-51 (19, 25), here we compared the *ex vivo* anti-HIV activities of diverse fusion inhibitors (Fig. 7D). Notably, the prodrug T-20 and its lipid

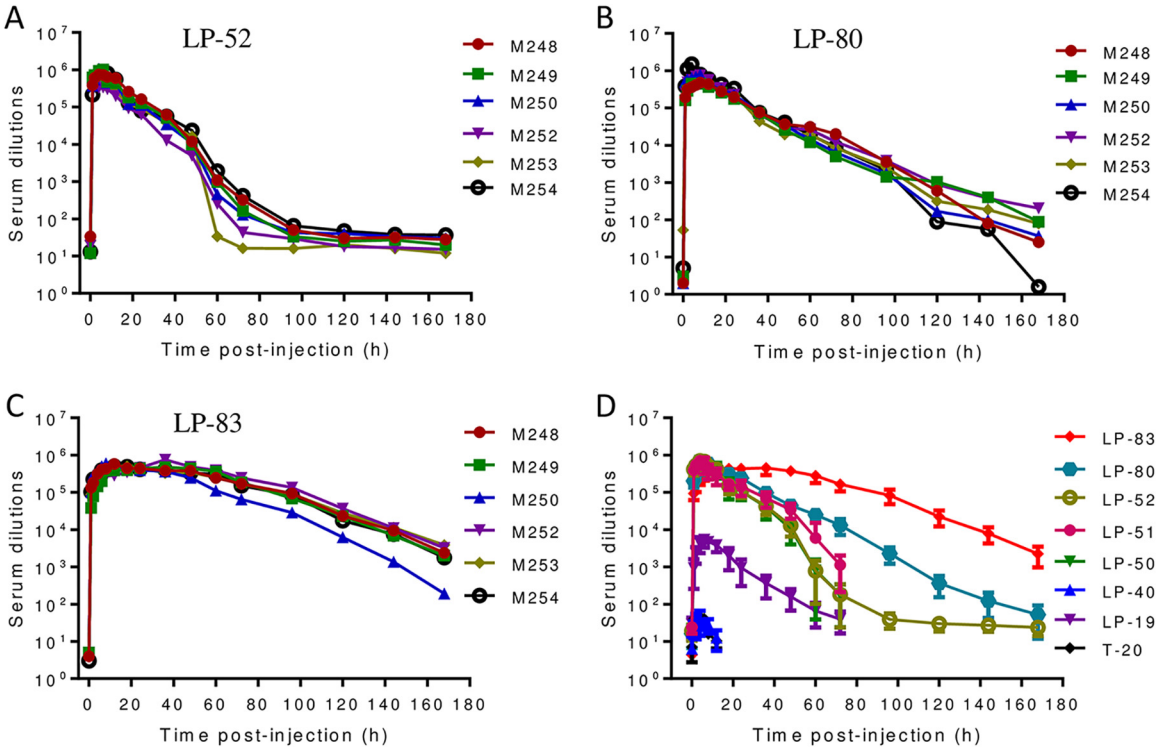

FIG 7 *Ex vivo* anti-HIV activities of lipopeptide fusion inhibitors. Each inhibitor (LP-52, LP-80, and LP-83) was subcutaneously injected into six rhesus monkeys at 3 mg/kg, and monkey sera were harvested at different time points before and after injection. The inhibitory activities of sera from monkeys administered LP-52 (A), LP-80 (B), and LP-83 (C) on HIV-1_{NL4-3} were measured by a single-cycle infection assay, and serum dilutions required for 50% inhibition of virus infection were calculated. (D) Comparison of HIV-inhibitory activities in the monkey sera containing different inhibitors. Since the same group of monkeys was used, the data for T-20, LP-19, LP-40, LP-50, and LP-51 were obtained from previous studies (19, 25).

derivative LP-40 only showed serum antiviral peaks of ~40-fold dilution, and their anti-HIV activities were not detected 6 h after injection. Therefore, the present results suggested that LP-83 possesses extremely potent and long-lasting *in vivo* antiviral activities, being >10,000-fold more active than T-20.

DISCUSSION

In this study, we have generated a group of cholesterol-conjugated fusion inhibitors and characterized their structural and functional properties in comparison to the fatty acid-conjugated lipopeptides developed previously. As shown, the cholesterylated inhibitors, such as LP-83 and LP-86, possess the most potent activities in inhibiting divergent HIV-1, HIV-2, and SIV isolates; especially, they show dramatically increased potencies on T-20-resistant mutants that still render high cross-resistance to the fatty acid derivatives. From different angles, we have further explored the mechanisms underlying the antiviral activities of the newly developed lipopeptides, including their inhibitions on Env-mediated cell-cell fusion and binding abilities with the cell and viral membranes and human serum albumin (HSA), as well as the cytotoxicity. Furthermore, we have demonstrated the extremely potent and long-lasting anti-HIV activity of LP-83 in rhesus monkeys. Taken together, the present studies have provided novel fusion inhibitor candidates for clinical development and offered important tools to elucidate the mechanisms of viral fusion and inhibition.

HIV entry occurs within the cell membrane domain known as "lipid rafts," where cholesterol and sphingolipid are enriched (34–36). A substantial body of evidence supports the importance of cholesterol and sphingolipid in HIV entry (34, 36–39). Notably, CD4, the primary receptor for HIV, is particularly enriched in the lipid rafts, and the fusion protein gp41 can associate with caveolin-1, a cholesterol-binding protein in the lipid rafts called caveolae (40, 41). Thus, cholesterol is enriched in caveolae and lies

together with HIV particles. The lipid membrane of HIV has a different lipid composition than the cell membrane, being particularly enriched in cholesterol and sphingomyelin, which likely results from the high-order complexes in confined areas of the interacting viral-host membranes (42, 43). It has long been recognized that targeting a drug to a membrane to increase its binding affinity toward membrane-bound receptors thereby improves its pharmaceutical profiles, including the inhibitory activity and pharmacokinetics. For viral fusion inhibitor peptides, and T-20 in particular, a number of examples document the general advantage of this strategy. For example, genetically anchoring T-20 to the cell membrane efficiently increases its antiviral activity (44, 45). Importantly, mutations in the C-terminal tryptophan-rich motif (TRM) of T-20, which completely inactivated the free peptide, did not reduce the potency of the membrane anchored one (44). It was found that the addition of a C-terminal octyl group to T-20 increased its inhibitory potency, and octylation rescued the activity of the inactive mutant, in which four C-terminal residues were substituted (21).

Because of the critical roles of cholesterol-enriched lipid rafts in HIV entry, Ingallinella and colleagues proposed that cholesterol might serve as an ideal anchor to localize stably a peptide to a lipid membrane (17). By conjugating a cholesterol group via a flexible linker and a cysteine residue to the C terminus of C34, the authors prepared the lipopeptide C34-Chol, which was 25- to 100-fold more potent than C34, and 50- to 400-fold more potent than T-20, considered as the most potent HIV fusion inhibitor to date (17). Indeed, C34-Chol was shown to interact preferentially with cholesterol-rich liquid-ordered membranes, mimicking biological membrane lipid rafts, as well as with human erythrocytes and PBMCs (46). Since then, the cholesterol conjugation strategy has been widely applied to develop fusion inhibitors against diverse enveloped viruses, including influenza virus (47), parainfluenza virus (33), Hendra virus (33), Nipah virus (48), Ebola virus (49), measles virus (50), SV5 (33), Newcastle disease virus (NDV) (51), and infectious bronchitis virus (51). In all the cases, the cholesterol-conjugated fusion inhibitors displayed 50- to 100-fold improvements over the template peptides (52). In sharp contrast, here we show that the potency of the cholesterylated inhibitor LP-83 was increased 7,059-fold over that of its template peptide (P-52), which was determined previously with the same panel of 36 HIV-1 isolates (26). In comparison, LP-83 was 11,937-fold more active than T-20 and 22-fold more active than C34-Chol (Table 2). More strikingly, the truncated template peptides for LP-93 (25-mer), LP-94 (24-mer), and LP-95 (21-mer) were inactive or very weak inhibitors (26); however, the cholesterol conjugation created the short lipopeptides that inhibited divergent HIV-1 subtypes at very low picomolar concentrations. For example, LP-93 was still 5,311-fold more potent than T-20 and 10-fold more potent than C34-Chol. LP-83 and LP-86 are composed of 29 amino acids, being a much smaller size with respect to T-20 (36-mer) and C34-Chol (38-mer), which also highlights their advantages as a drug candidate. Very importantly, the present studies have again verified the core sequence for designing an extremely potent and broad HIV fusion inhibitor and the target site of viral vulnerability, the concepts we proposed previously (26).

From the present studies, several additional critical findings should be highlighted. First, LP-83 and LP-86 share the same template with the C_{16} fatty acid-conjugated inhibitors LP-51/52 and the C_{18} fatty acid-conjugated inhibitor LP-80; however, we found that LP-83 and LP-86 were much more efficient than the fatty acid derivatives in inhibiting different T-20-resistant mutant viruses (Table 3). How a specific lipid anchor can change the binding and inhibitory activities of the inhibitors remains to be characterized, which might reveal new insights into the mechanisms of viral fusion and inhibition. Second, the new cholesterylated inhibitors were highly effective in blocking HIV Env-mediated cell-cell fusion. Very interestingly, while the C- or N-terminally truncated lipopeptides LP-93 and LP-94 sustained the very potent inhibitory activities, the minimum lipopeptide LP-95, which was truncated from both the N and C terminals, exhibited a greatly increased potency on the cell-cell fusion. It would also be intriguing to know whether a relatively small size would benefit the fusion inhibitor to overcome

the steric hindrance that occurred during the cell-cell contact. Considering that HIV infects various cells and tissues *in vivo*, the minimum inhibitor LP-95 might offer an advantage regarding tissue penetration. Especially, it was reported that a cholesterylated peptide fusion inhibitor against measles virus was able to penetrate the brain barrier to distribute within the central nervous system (CNS) (50). However, T-20 was shown to have a negligible distribution in the CNS, which precluded its use for HIV dementia and encephalitis (53). Thus, the brain-penetrating capacity of cholesterylated peptides is also a key feature that supports their further development as HIV therapeutics. Third, the present studies verified the membrane-anchoring capacity of lipopeptides, which can concentrate the inhibitors at the local site where fusion occurs. Very promisingly, the lipopeptide inhibitors can also interact and bind to the viral membranes and exert their antiviral functionality. It was reported that a recombinant protein containing a fusion inhibitor peptide (T1144) resulted in rapid inactivation of HIV virions (54). Recently, Nieto-Garai et al. identified three lipidomimetic compounds that bound to the viral membrane and inhibited virus entry by altering viral membrane order (55). Therefore, we wonder whether a membrane-bound lipopeptide inhibitor can bind to and destabilize the viral lipid composition to directly inactivate HIV in the absence of the target cells. Considering that most currently approved anti-HIV drugs (e.g., reverse transcriptase inhibitors, protease inhibitors, and entry inhibitors) must act inside or on the surface of the target cell but none can inactivate virions away from cells, novel therapeutics that can actively attack the virus in circulation before it attaches to the target cell would provide additional advantages. Fourth, because of its low anti-HIV activity and short half-life, T-20 requires a large dosage (90 mg, twice daily). Herein, the cholesterylated LP-83 was shown possessing extremely potent and long-acting anti-HIV activity in the monkeys. While the fatty acid-modified LP-52 and LP-80 might be used once daily or twice weekly, our present data support a once-a-week protocol for LP-83, which is indeed the case for C34-Chol in humans (28). Fifth, the druggability of LP-83 was also validated by its low cytotoxicity and strong binding capacity with HSA. Intriguingly, the binding of lipopeptides with HSA did not affect their anti-HIV activity. Taking all the findings together, we conclude that a cholesterol-based lipopeptide inhibitor has prominent advantages over the fatty acid derivatives. In our future studies, we would like to address the following aspects. First, what are the structural properties of the lipopeptide inhibitors in the presence and absence of a target surrogate? It would be valuable to define whether they form micelles or other superstructures that might interfere with HIV infection in a different way from the inhibition of 6-HB formation. Second, how can we explain that the lipopeptides were not depleted from the rhesus monkey plasma by membrane binding and accumulation in tissues? One may speculate that the binding might be reversible, thus determining the pharmacokinetics of serum lipopeptides. Third, it is highly critical to select and characterize lipopeptide-resistant HIV mutant viruses, which will definitely help to clarify the modes of action of the inhibitors. Therefore, the present works have not only delivered new drug candidates for clinical development but also offered important reagents to investigate the mechanisms of HIV entry and its inhibition.

MATERIALS AND METHODS

Cell lines and reagents. HEK293T, MT-4, C8166, and U937 cells were purchased from the American Type Culture Collection (ATCC, Rockville, MD). The following reagents were obtained through the AIDS Reagent Program, Division of AIDS, NIAID, NIH: TZM-bl cells from John C. Kappes and Xiaoyun Wu, the panel of global HIV-1 Env clones from David Montefiori, molecular HIV-1_{NL4-3} clone from Malcolm Martin, HIV-1_{JRCSF} clone from Irvin S. Y. Chen and Yoshio Koyanagi, HIV-$1_{89.6}$ clone from Ronald G. Collman, HIV-2_{ST} clone from Beatrice Hahn and George Shaw, and HIV-2_{ROD} clone from the Centre for AIDS Reagents, NIBSC, UK. Two plasmids encoding SIV Envs (pSIVpbj-Env and pSIV239-Env) were kindly provided by Jianqing Xu at the Shanghai Public Health Clinical Center, Fudan University, China. The plasmid expressing DSP_{1-7} and 293FT cells stably expressing CXCR4/CCR5 and DSP_{8-11} were provided by Zene Matsuda at the Institute of Medical Science of the University of Tokyo (Tokyo, Japan).

Peptide synthesis and lipid conjugation. Peptides were synthesized on rink amide 4-methylbenzhydrylamine (MBHA) resin using a standard solid-phase 9-fluorenylmethoxycarbonyl (FMOC) method as described previously (18). For fatty acid conjugation, the template peptide contained a C-terminal lysine residue with a 1-(4,4-dimethyl-2,6-dioxocyclohexylidene)ethyl (Dde) side chain-

protecting group, enabling the conjugation of a C_{16} or C_{18} fatty acid group that requires a deprotection step in a solution of 2% hydrazine hydrate-*N,N*-dimethylformamide (DMF); the cholesterylated peptides LP-83, LP-86, and C34-Chol were prepared by chemoselective thioether conjugation between a template peptide containing a C-terminal cysteine residue and bromoacetic acid cholesterol. The cholesterylated peptides LP-93, LP-94, and LP-95 were alternatively synthesized by conjugating cholesteryl chloroformate to the C-terminal lysine residue. All peptides were N-terminally acetylated and C-terminally amidated, and they were purified by reverse-phase high-performance liquid chromatography (HPLC) to more than 95% homogeneity, followed by characterization with mass spectrometry.

Circular dichroism spectroscopy. The α-helicity and thermostability of lipopeptide inhibitors in the presence or absence of a target mimic peptide (N39) were determined by CD spectroscopy as described previously (56). Briefly, an inhibitor was diluted in phosphate-buffered saline (PBS; pH 7.2) and incubated at 37°C for 30 min in the presence or absence of an equal molar concentration of N39. CD spectra were collected on a Jasco spectropolarimeter (model J-815) using a 1-nm bandwidth with a 1 -nm step resolution from 195 to 270 nm at room temperature. Spectra were corrected by subtracting a solvent blank. The α-helical content was calculated from the CD signal by dividing the mean residue ellipticity [θ] at 222 nm, with a value of $-33{,}000$ deg cm^2 dmol^{-1} corresponding to 100% helix. Thermal denaturation was performed by monitoring the ellipticity change at 222 nm from 20°C to 98°C at a rate of 2°C/min, and melting temperature (T_m) was defined as the midpoint of the thermal unfolding transition.

Antiviral activity of fusion inhibitors. Inhibitory activity of inhibitors on three replication-competent HIV-1 (NL4-3, JR-CSF, and 89.6) and two HIV-2 (ROD and ST) isolates was determined as described previously (25). Briefly, viral stocks were prepared by transfecting viral molecular clones into HEK293T cells. Culture supernatants were harvested 48 h posttransfection, and 50% tissue culture infectious dose ($TCID_{50}$) was measured in TZM-bl cells. An inhibitor was prepared in 3-fold dilutions, mixed with 100 $TCID_{50}$ of viruses, and then incubated 1 h at room temperature. One hundred microliters of the mixture was added to TZM-bl cells (10^4/well in a 100 μl volume) and incubated for 48 h at 37°C. The cells were harvested and lysed in reporter lysis buffer, and luciferase activity was measured using luciferase assay reagents and a luminescence counter (Promega, Madison, WI, USA).

The inhibitory activity of inhibitors on a panel of HIV-1 subtypes and two SIV isolates was determined by a pseudovirus-based single-cycle infection assay as described previously (25). Pseudoviruses were generated by cotransfecting HEK293T cells with an Env-expressing plasmid and a backbone plasmid (pSG3Δenv) that encodes an Env-defective luciferase-expressing HIV-1 genome. Culture supernatants were harvested 48 h after transfection, and $TCID_{50}$ was determined in TZM-bl cells. Similar to that described above, a total of 100 $TCID_{50}$ viruses were used to infect TZM-bl cells in the presence or absence of serially 3-fold diluted inhibitors. Cells were harvested 2 days postinfection, and luciferase activity was measured with luciferase assay reagents. The 50% inhibitory concentration (IC_{50}) was calculated as the final cell culture concentration of an inhibitor that caused a 50% reduction in relative luminescence units (RLUs) compared to the level of the virus control subtracted from that of the cell control.

Inhibition of HIV-1 Env-mediated cell-cell fusion. Inhibitory activity of inhibitors on Env-mediated cell-cell fusion was measured by a dual-split-protein (DSP)-based assay as described previously (57–59). Briefly, a total of 1.5×10^4 293T cells (effector cells) were plated in a 96-well plate and incubated at 37°C. On the next day, 293T cells were cotransfected with an Env-expressing plasmid and a DSP_{1-7} plasmid and incubated 24 h at 37°C. 293FT cells stably expressing CXCR4/CCR5 and DSP_{8-11} (target cells) were resuspended and EnduRen live cell substrate (Promega) was added, followed by incubation for 30 min at 37°C. Then, the target cells (3×10^4/well) were cocultured with effector cells at 37°C in the presence or absence of a tested inhibitor at graded concentrations. The mixed cells were then spun down to maximize cell-cell contact and incubated for 1 h at 37°C. Luciferase activity was measured with luciferase assay reagents and IC_{50} values were calculated as described above.

Binding ability of lipopeptide inhibitors with cellular membrane. To determine the binding ability of inhibitors with the target cell membrane, TZM-bl cells were plated in a 96-well plate (10^4/well) and incubated at 37°C overnight. A diluted inhibitor was added to the cells and incubated 1 h at 37°C. The cells were thoroughly washed with PBS, followed by the addition of 100 $TCID_{50}$ of infectious HIV-1_{NL4-3} or HIV-1_{JRCSF}. After 2 days of culture, the inhibitory activity of the inhibitors that survived the washing steps was determined by luciferase assay reagents. To physically visualize the inhibitors that bound to the cell membrane, an inhibitor was N-terminally labeled with fluorescein isothiocyanate (FITC). TZM-bl cells (10^5/well) were plated on coverslips and incubated at 37°C overnight. A FITC-labeled inhibitor was diluted and added to the cells, followed by incubation at 37°C for 30 min. TZM-bl cells were then fixed for 15 min with 4% paraformaldehyde and washed three times with PBS. Images were captured with a laser confocal microscope.

Binding ability of lipopeptide inhibitors with viral membrane. To determine the binding ability of inhibitors with the HIV-1 membrane, a polyethylene glycol (PEG) 6000-based method was used to separate the virus particles from the inhibitors as described previously (54, 60). In brief, a diluted inhibitor was added to 200 $TCID_{50}$ of HIV-1_{NL4-3} or HIV-1_{JRCSF} and incubated 1 h at 4°C. Then, 3% PEG 6000 was added to the virus and incubated 1 h at 4°C. The mixture was centrifuged on a microcentrifuge at 14,000 rpm for 40 min, and the supernatants were removed. The virus pellet was washed two times with 1 ml of 3% PEG 6000 containing 10 mg/ml bovine serum albumin (BSA) and then resuspended in 100 μl of Dulbecco's modified Eagle medium (DMEM). The inhibitor-treated virus was mixed with 100 μl of TZM-bl cells (1×10^5/ml) to start the infection. After 2 days of culture, the inhibitory activity of the viral membrane-bound inhibitors was determined by luciferase assay reagents.

Binding ability of lipopeptide inhibitors with HSA. The binding ability of cholesterylated inhibitors and controls with human serum albumin (HSA) was determined by an enzyme-linked immunosorbent

assay (ELISA) described previously (26). Briefly, 5% HSA in 0.1 M carbonate buffer (pH 9.6) was coated on a 96-well polystyrene plate at 4°C overnight. After three washings, an inhibitor was added to the wells and incubated at 37°C for 1 h, followed by three washes with PBS-T (PBS containing 0.1% Tween 20). Then, the mouse monoclonal antibody 12H1, which was developed against the template peptide P-52 in our laboratory, was added and incubated 1 h at 37°C. After washes with PBS-T, horseradish peroxidase (HRP)-conjugated rabbit anti-mouse IgG was added and incubated 1 h at 37°C. The reaction was visualized by adding 3,3,5,5-tetramethylbenzidine (TMB) substrate, and absorbance at 450 nm (A_{450}) was measured by an ELISA plate reader (Bio-Rad Laboratories, Hercules, CA, USA).

Cytotoxicity of LP-83. Cytotoxicity of LP-83 on diverse cell lines (TZM-bl, MT-4, C8166, U937, and HEK293T) and human PBMCs was measured using a CellTiter 96 AQueous One Solution cell proliferation assay (Promega). In brief, a total of 1×10^4 cells were seeded on a 96-well tissue culture plate, and 50 μl of LP-83 diluted at graded concentrations was added to the cells. After incubation at 37°C for 2 days, 20 μl of CellTiter 96 AQueous One Solution reagent was pipetted into each well and incubated 2 h at 37°C. The absorbance was measured at 490 nm using a SpectraMax M5 microplate reader (Molecular Devices, San Jose, CA, USA), and cell viability (percentage) and 50% cytotoxic concentration (CC_{50}) were calculated.

***Ex vivo* antiviral activities of lipopeptide inhibitors in rhesus monkeys.** We previously adapted a simple and sensitive system for evaluating the antiviral activities of various HIV fusion inhibitors without animal infection facilities (18, 19, 25, 61). In this study, the *ex vivo* anti-HIV activities of three newly developed lipopeptides (LP-52, LP-80, and LP-83) were determined in a nonhuman primate model. In brief, an inhibitor (3 mg/kg of body weight) was subcutaneously administered to six Chinese rhesus macaques who were previously used for evaluating the anti-HIV activities of T-20, LP-19, LP-50, and LP-51 (19, 25). Similarly, serum samples of macaques were harvested before injection (0 h) and after injection (1, 2, 4, 6, 8, 12, 18, 24, 36, 48, 60, and 72 h), and their inhibitory activities on HIV-1_{NL4-3} were measured by a single-cycle infection assay. The 50% effective concentration was defined as the fold serum dilution that inhibited 50% of virus infection.

ACKNOWLEDGMENTS

We thank Zene Matsuda at the Institute of Medical Science, University of Tokyo, for providing plasmids and cells for the DSP-based cell-cell fusion assay and Jianqing Xu at the Shanghai Public Health Clinical Center and Institutes of Biomedical Sciences of Fudan University for providing the plasmids encoding SIV Env.

This work was supported by grants from the National Natural Science Foundation of China (81630061), National Science and Technology Major Project of China (2018ZX10301103), and CAMS Innovation Fund for Medical Sciences (2017-I2M-1-014).

REFERENCES

1. Eckert DM, Kim PS. 2001. Mechanisms of viral membrane fusion and its inhibition. Annu Rev Biochem 70:777–810. https://doi.org/10.1146/annurev.biochem.70.1.777.
2. Chan DC, Kim PS. 1998. HIV entry and its inhibition. Cell 93:681–684. https://doi.org/10.1016/S0092-8674(00)81430-0.
3. Este JA, Telenti A. 2007. HIV entry inhibitors. Lancet 370:81–88. https://doi.org/10.1016/S0140-6736(07)61052-6.
4. Lobritz MA, Ratcliff AN, Arts EJ. 2010. HIV-1 entry, inhibitors, and resistance. Viruses 2:1069–1105. https://doi.org/10.3390/v2051069.
5. Eggink D, Berkhout B, Sanders RW. 2010. Inhibition of HIV-1 by fusion inhibitors. Curr Pharm Des 16:3716–3728. https://doi.org/10.2174/138161210794079218.
6. He Y. 2013. Synthesized peptide inhibitors of HIV-1 gp41-dependent membrane fusion. Curr Pharm Des 19:1800–1809. https://doi.org/10.2174/1381612811319100004.
7. Lalezari JP, Henry K, O'Hearn M, Montaner JS, Piliero PJ, Trottier B, Walmsley S, Cohen C, Kuritzkes DR, Eron JJ, Jr, Chung J, DeMasi R, Donatacci L, Drobnes C, Delehanty J, Salgo M, TORO1 Study Group. 2003. Enfuvirtide, an HIV-1 fusion inhibitor, for drug-resistant HIV infection in North and South America. N Engl J Med 348:2175–2185. https://doi.org/10.1056/NEJMoa035026.
8. Flexner C. 2007. HIV drug development: the next 25 years. Nat Rev Drug Discov 6:959–966. https://doi.org/10.1038/nrd2336.
9. Kilby JM, Hopkins S, Venetta TM, DiMassimo B, Cloud GA, Lee JY, Alldredge L, Hunter E, Lambert D, Bolognesi D, Matthews T, Johnson MR, Nowak MA, Shaw GM, Saag MS. 1998. Potent suppression of HIV-1 replication in humans by T-20, a peptide inhibitor of gp41-mediated virus entry. Nat Med 4:1302–1307. https://doi.org/10.1038/3293.
10. Chan DC, Chutkowski CT, Kim PS. 1998. Evidence that a prominent cavity in the coiled coil of HIV type 1 gp41 is an attractive drug target. Proc Natl Acad Sci U S A 95:15613–15617. https://doi.org/10.1073/pnas.95.26.15613.
11. He Y, Xiao Y, Song H, Liang Q, Ju D, Chen X, Lu H, Jing W, Jiang S, Zhang L. 2008. Design and evaluation of sifuvirtide, a novel HIV-1 fusion inhibitor. J Biol Chem 283:11126–11134. https://doi.org/10.1074/jbc.M800200200.
12. Otaka A, Nakamura M, Nameki D, Kodama E, Uchiyama S, Nakamura S, Nakano H, Tamamura H, Kobayashi Y, Matsuoka M, Fujii N. 2002. Remodeling of gp41-C34 peptide leads to highly effective inhibitors of the fusion of HIV-1 with target cells. Angew Chem Int Ed Engl 41:2937–2940. https://doi.org/10.1002/1521-3773(20020816)41:16<2937::AID-ANIE2937>3.0.CO;2-J.
13. Dwyer JJ, Wilson KL, Davison DK, Freel SA, Seedorff JE, Wring SA, Tvermoes NA, Matthews TJ, Greenberg ML, Delmedico MK. 2007. Design of helical, oligomeric HIV-1 fusion inhibitor peptides with potent activity against enfuvirtide-resistant virus. Proc Natl Acad Sci U S A 104:12772–12777. https://doi.org/10.1073/pnas.0701478104.
14. Chong H, Yao X, Qiu Z, Sun J, Zhang M, Waltersperger S, Wang M, Liu SL, Cui S, He Y. 2013. Short-peptide fusion inhibitors with high potency against wild-type and enfuvirtide-resistant HIV-1. FASEB J 27:1203–1213. https://doi.org/10.1096/fj.12-222547.
15. Chong H, Qiu Z, Su Y, Yang L, He Y. 2015. Design of a highly potent HIV-1 fusion inhibitor targeting the gp41 pocket. AIDS 29:13–21. https://doi.org/10.1097/QAD.0000000000000498.
16. Xiong S, Borrego P, Ding X, Zhu Y, Martins A, Chong H, Taveira N, He Y. 2017. A helical short-peptide fusion inhibitor with highly potent activity against human immunodeficiency virus type 1 (HIV-1), HIV-2, and simian immunodeficiency virus. J Virol 91:e01839-16. https://doi.org/10.1128/JVI.01839-16.
17. Ingallinella P, Bianchi E, Ladwa NA, Wang YJ, Hrin R, Veneziano M, Bonelli F, Ketas TJ, Moore JP, Miller MD, Pessi A. 2009. Addition of a cholesterol

group to an HIV-1 peptide fusion inhibitor dramatically increases its antiviral potency. Proc Natl Acad Sci U S A 106:5801–5806. https://doi.org/10.1073/pnas.0901007106.
18. Chong H, Wu X, Su Y, He Y. 2016. Development of potent and long-acting HIV-1 fusion inhibitors. AIDS 30:1187–1196. https://doi.org/10.1097/QAD.0000000000001073.
19. Chong H, Xue J, Xiong S, Cong Z, Ding X, Zhu Y, Liu Z, Chen T, Feng Y, He L, Guo Y, Wei Q, Zhou Y, Qin C, He Y. 2017. A lipopeptide HIV-1/2 fusion inhibitor with highly potent *in vitro*, *ex vivo*, and *in vivo* antiviral activity. J Virol 91:e00288-17. https://doi.org/10.1128/JVI.00288-17.
20. Wexler-Cohen Y, Shai Y. 2007. Demonstrating the C-terminal boundary of the HIV 1 fusion conformation in a dynamic ongoing fusion process and implication for fusion inhibition. FASEB J 21:3677–3684. https://doi.org/10.1096/fj.07-8582com.
21. Peisajovich SG, Gallo SA, Blumenthal R, Shai Y. 2003. C-terminal octylation rescues an inactive T20 mutant: implications for the mechanism of HIV/SIMIAN immunodeficiency virus-induced membrane fusion. J Biol Chem 278:21012–21017. https://doi.org/10.1074/jbc.M212773200.
22. Kliger Y, Gallo SA, Peisajovich SG, Munoz-Barroso I, Avkin S, Blumenthal R, Shai Y. 2001. Mode of action of an antiviral peptide from HIV-1. Inhibition at a post-lipid mixing stage. J Biol Chem 276:1391–1397. https://doi.org/10.1074/jbc.M004113200.
23. Zhang X, Ding X, Zhu Y, Chong H, Cui S, He J, Wang X, He Y. 2019. Structural and functional characterization of HIV-1 cell fusion inhibitor T20. AIDS 33:1–11. https://doi.org/10.1097/QAD.0000000000001979.
24. Ding X, Zhang X, Chong H, Zhu Y, Wei H, Wu X, He J, Wang X, He Y. 2017. Enfuvirtide (T20)-based lipopeptide is a potent HIV-1 cell fusion inhibitor: implication for viral entry and inhibition. J Virol 91:e00831-17. https://doi.org/10.1128/JVI.00831-17.
25. Chong H, Xue J, Zhu Y, Cong Z, Chen T, Guo Y, Wei Q, Zhou Y, Qin C, He Y. 2018. Design of novel HIV-1/2 fusion inhibitors with high therapeutic efficacy in rhesus monkey models. J Virol 92:e00775-18. https://doi.org/10.1128/JVI.00775-18.
26. Chong H, Zhu Y, Yu D, He Y. 2018. Structural and functional characterization of membrane fusion inhibitors with extremely potent activity against HIV-1, HIV-2, and simian immunodeficiency virus. J Virol 92:e01088-18. https://doi.org/10.1128/JVI.01088-18.
27. Chong H, Xue J, Zhu Y, Cong Z, Chen T, Wei Q, Qin C, He Y. 2019. Monotherapy with a low-dose lipopeptide HIV fusion inhibitor maintains long-term viral suppression in rhesus macaques. PLoS Pathog 15:e1007552. https://doi.org/10.1371/journal.ppat.1007552.
28. Quinn K, Traboni C, Penchala SD, Bouliotis G, Doyle N, Libri V, Khoo S, Ashby D, Weber J, Nicosia A, Cortese R, Pessi A, Winston A. 2017. A first-in-human study of the novel HIV-fusion inhibitor C34-PEG4-Chol. Sci Rep 7:9447. https://doi.org/10.1038/s41598-017-09230-0.
29. deCamp A, Hraber P, Bailer RT, Seaman MS, Ochsenbauer C, Kappes J, Gottardo R, Edlefsen P, Self S, Tang H, Greene K, Gao H, Daniell X, Sarzotti-Kelsoe M, Gorny MK, Zolla-Pazner S, LaBranche CC, Mascola JR, Korber BT, Montefiori DC. 2014. Global panel of HIV-1 Env reference strains for standardized assessments of vaccine-elicited neutralizing antibodies. J Virol 88:2489–2507. https://doi.org/10.1128/JVI.02853-13.
30. Ashkenazi A, Viard M, Unger L, Blumenthal R, Shai Y. 2012. Sphingopeptides: dihydrosphingosine-based fusion inhibitors against wild-type and enfuvirtide-resistant HIV-1. FASEB J 26:4628–4636. https://doi.org/10.1096/fj.12-215111.
31. Wexler-Cohen Y, Shai Y. 2009. Membrane-anchored HIV-1 N-heptad repeat peptides are highly potent cell fusion inhibitors via an altered mode of action. PLoS Pathog 5:e1000509. https://doi.org/10.1371/journal.ppat.1000509.
32. Mathieu C, Porotto M, Figueira T, Horvat B, Moscona A. 2018. Fusion inhibitory lipopeptides engineered for prophylaxis of Nipah virus in primates. J Infect Dis 218:218–227. https://doi.org/10.1093/infdis/jiy152.
33. Porotto M, Yokoyama CC, Palermo LM, Mungall B, Aljofan M, Cortese R, Pessi A, Moscona A. 2010. Viral entry inhibitors targeted to the membrane site of action. J Virol 84:6760–6768. https://doi.org/10.1128/JVI.00135-10.
34. Waheed AA, Freed EO. 2010. The role of lipids in retrovirus replication. Viruses 2:1146–1180. https://doi.org/10.3390/v2051146.
35. Campbell SM, Crowe SM, Mak J. 2001. Lipid rafts and HIV-1: from viral entry to assembly of progeny virions. J Clin Virol 22:217–227. https://doi.org/10.1016/S1386-6532(01)00193-7.
36. Leung K, Kim JO, Ganesh L, Kabat J, Schwartz O, Nabel GJ. 2008. HIV-1 assembly: viral glycoproteins segregate quantally to lipid rafts that associate individually with HIV-1 capsids and virions. Cell Host Microbe 3:285–292. https://doi.org/10.1016/j.chom.2008.04.004.
37. Aloia RC, Tian H, Jensen FC. 1993. Lipid composition and fluidity of the human immunodeficiency virus envelope and host cell plasma membranes. Proc Natl Acad Sci U S A 90:5181–5185. https://doi.org/10.1073/pnas.90.11.5181.
38. Aloia RC, Jensen FC, Curtain CC, Mobley PW, Gordon LM. 1988. Lipid composition and fluidity of the human immunodeficiency virus. Proc Natl Acad Sci U S A 85:900–904. https://doi.org/10.1073/pnas.85.3.900.
39. Viard M, Parolini I, Sargiacomo M, Fecchi K, Ramoni C, Ablan S, Ruscetti FW, Wang JM, Blumenthal R. 2002. Role of cholesterol in human immunodeficiency virus type 1 envelope protein-mediated fusion with host cells. J Virol 76:11584–11595. https://doi.org/10.1128/JVI.76.22.11584-11595.2002.
40. Hovanessian AG, Briand JP, Said EA, Svab J, Ferris S, Dali H, Muller S, Desgranges C, Krust B. 2004. The caveolin-1 binding domain of HIV-1 glycoprotein gp41 is an efficient B cell epitope vaccine candidate against virus infection. Immunity 21:617–627. https://doi.org/10.1016/j.immuni.2004.08.015.
41. Benferhat R, Martinon F, Krust B, Le Grand R, Hovanessian AG. 2009. The CBD1 peptide corresponding to the caveolin-1 binding domain of HIV-1 glycoprotein gp41 elicits neutralizing antibodies in cynomolgus macaques when administered with the tetanus T helper epitope. Mol Immunol 46:705–712. https://doi.org/10.1016/j.molimm.2008.10.001.
42. Brugger B, Glass B, Haberkant P, Leibrecht I, Wieland FT, Krausslich HG. 2006. The HIV lipidome: a raft with an unusual composition. Proc Natl Acad Sci U S A 103:2641–2646. https://doi.org/10.1073/pnas.0511136103.
43. Lorizate M, Sachsenheimer T, Glass B, Habermann A, Gerl MJ, Krausslich HG, Brugger B. 2013. Comparative lipidomics analysis of HIV-1 particles and their producer cell membrane in different cell lines. Cell Microbiol 15:292–304. https://doi.org/10.1111/cmi.12101.
44. Hildinger M, Dittmar MT, Schult-Dietrich P, Fehse B, Schnierle BS, Thaler S, Stiegler G, Welker R, von Laer D. 2001. Membrane-anchored peptide inhibits human immunodeficiency virus entry. J Virol 75:3038–3042. https://doi.org/10.1128/JVI.75.6.3038-3042.2001.
45. Egelhofer M, Brandenburg G, Martinius H, Schult-Dietrich P, Melikyan G, Kunert R, Baum C, Choi I, Alexandrov A, von Laer D. 2004. Inhibition of human immunodeficiency virus type 1 entry in cells expressing gp41-derived peptides. J Virol 78:568–575. https://doi.org/10.1128/JVI.78.2.568-575.2004.
46. Augusto MT, Hollmann A, Castanho MA, Porotto M, Pessi A, Santos NC. 2014. Improvement of HIV fusion inhibitor C34 efficacy by membrane anchoring and enhanced exposure. J Antimicrob Chemother 69:1286–1297. https://doi.org/10.1093/jac/dkt529.
47. Lee KK, Pessi A, Gui L, Santoprete A, Talekar A, Moscona A, Porotto M. 2011. Capturing a fusion intermediate of influenza hemagglutinin with a cholesterol-conjugated peptide, a new antiviral strategy for influenza virus. J Biol Chem 286:42141–42149. https://doi.org/10.1074/jbc.M111.254243.
48. Porotto M, Rockx B, Yokoyama CC, Talekar A, Devito I, Palermo LM, Liu J, Cortese R, Lu M, Feldmann H, Pessi A, Moscona A. 2010. Inhibition of Nipah virus infection *in vivo*: targeting an early stage of paramyxovirus fusion activation during viral entry. PLoS Pathog 6:e1001168. https://doi.org/10.1371/journal.ppat.1001168.
49. Higgins CD, Koellhoffer JF, Chandran K, Lai JR. 2013. C-peptide inhibitors of Ebola virus glycoprotein-mediated cell entry: effects of conjugation to cholesterol and side chain-side chain crosslinking. Bioorg Med Chem Lett 23:5356–5360. https://doi.org/10.1016/j.bmcl.2013.07.056.
50. Welsch JC, Talekar A, Mathieu C, Pessi A, Moscona A, Horvat B, Porotto M. 2013. Fatal measles virus infection prevented by brain-penetrant fusion inhibitors. J Virol 87:13785–13794. https://doi.org/10.1128/JVI.02436-13.
51. Li CG, Tang W, Chi XJ, Dong ZM, Wang XX, Wang XJ. 2013. A cholesterol tag at the N terminus of the relatively broad-spectrum fusion inhibitory peptide targets an earlier stage of fusion glycoprotein activation and increases the peptide's antiviral potency *in vivo*. J Virol 87:9223–9232. https://doi.org/10.1128/JVI.01153-13.
52. Pessi A. 2015. Cholesterol-conjugated peptide antivirals: a path to a rapid response to emerging viral diseases. J Pept Sci 21:379–386. https://doi.org/10.1002/psc.2706.
53. Price RW, Parham R, Kroll JL, Wring SA, Baker B, Sailstad J, Hoh R, Liegler T, Spudich S, Kuritzkes DR, Deeks SG. 2008. Enfuvirtide cerebrospinal

fluid (CSF) pharmacokinetics and potential use in defining CSF HIV-1 origin. Antivir Ther 13:369–374.
54. Lu L, Pan C, Li Y, Lu H, He W, Jiang S. 2012. A bivalent recombinant protein inactivates HIV-1 by targeting the gp41 prehairpin fusion intermediate induced by CD4 D1D2 domains. Retrovirology 9:104. https://doi.org/10.1186/1742-4690-9-104.
55. Nieto-Garai JA, Glass B, Bunn C, Giese M, Jennings G, Brankatschk B, Agarwal S, Börner K, Contreras FX, Knölker H-J, Zankl C, Simons K, Schroeder C, Lorizate M, Kräusslich H-G. 2018. Lipidomimetic compounds act as HIV-1 entry inhibitors by altering viral membrane structure. Front Immunol 9:1983. https://doi.org/10.3389/fimmu.2018.01983.
56. Chong H, Yao X, Qiu Z, Qin B, Han R, Waltersperger S, Wang M, Cui S, He Y. 2012. Discovery of critical residues for viral entry and inhibition through structural insight of HIV-1 fusion inhibitor CP621-652. J Biol Chem 287:20281–20289. https://doi.org/10.1074/jbc.M112.354126.
57. Ishikawa H, Meng F, Kondo N, Iwamoto A, Matsuda Z. 2012. Generation of a dual-functional split-reporter protein for monitoring membrane fusion using self-associating split GFP. Protein Eng Des Sel 25:813–820. https://doi.org/10.1093/protein/gzs051.
58. Kondo N, Miyauchi K, Meng F, Iwamoto A, Matsuda Z. 2010. Conformational changes of the HIV-1 envelope protein during membrane fusion are inhibited by the replacement of its membrane-spanning domain. J Biol Chem 285:14681–14688. https://doi.org/10.1074/jbc.M109.067090.
59. Zhang X, Zhu Y, Hu H, Zhang S, Wang P, Chong H, He J, Wang X, He Y. 2018. Structural insights into the mechanisms of action of short-peptide HIV-1 fusion inhibitors targeting the Gp41 pocket. Front Cell Infect Microbiol 8:51. https://doi.org/10.3389/fcimb.2018.00051.
60. Kutner RH, Zhang XY, Reiser J. 2009. Production, concentration and titration of pseudotyped HIV-1-based lentiviral vectors. Nat Protoc 4:495–505. https://doi.org/10.1038/nprot.2009.22.
61. Chong H, Qiu Z, Su Y, He Y. 2015. The N-terminal T-T motif of a third-generation HIV-1 fusion inhibitor is not required for binding affinity and antiviral activity. J Med Chem 58:6378–6388. https://doi.org/10.1021/acs.jmedchem.5b00109.